Epigallocatechin gallate (EGCG) with potent anti-*Helicobacter pylori* activity binds efficiently to its Histone like DNA binding protein

Ritu Raj[1,2], Nipanshu Agarwal[3], Sriram Raghavan[4], Tapati Chakraborti[2], Krishna Mohan Poluri[3], Gaurav Pande[5*] and Dinesh Kumar[1,*]

[1]*Centre of Biomedical Research (CBMR), SGPGIMS Campus, Raibareli Road, Lucknow-226014, Uttar Pradesh, India*

[2]*Department of Biochemistry & Biophysics, University of Kalyani, Kalyani-741235, West Bengal, India*

[3]*Department of Biotechnology and Centre for Nanotechnology Indian Institute of Technology Roorkee Roorkee – 247667, Uttarakhand, India*

[4]*Computational Structural Biology Team, RIKEN Center for Computational Science (R-CCS) Kobe-650-0047, Japan*

[5]*Department of Gastroeneterology, SGPGIMS, Lucknow-226014, Uttar Pradesh | India*

** Author for Correspondence:*

Dr. Gaurav Pande (DM, MBBS) Department of Gastroenterology, SGPGIMS, Raibareli Road, Lucknow-226014, Uttar Pradesh, India Email: drgauravpandey@yahoo.com Contact: +91-9170689999	Dr. Dinesh Kumar (Associate Professor) Centre of Biomedical Research (CBMR), SGPGIMS Campus, Raibareli Road, Lucknow-226014, Uttar Pradesh, India Email: dineshcbmr@gmail.com Contact: +91-8953261506

Keywords

Helicobacter pylori; Histone like DNA Binding Protein (Hup); Proton NMR; Molecular docking; Virtual screening; Molecular Dynamics simulation.

Figure S1: Geometry optimization performed for natural compound library containing anti-*Helicobacter pylori* (AHP) compounds (downloaded from the Pubchem database: https://pubchem.ncbi.nlm.nih.gov) using LigPrep(v2.3) application of Schrodinger [1] so that the Pka and protonation state of the compounds can be used to determine possible tautomerization in OPLS3 force field. The input library file contains 159 distinctive chemical compounds and the output file contains 246 conformations corresponding to 133 compounds with molecular weight less than 500 Da. The bond orders were optimised and ionization state of the ligands were generated with optimal pH of 7.0 using Epik(2.2). The display shown below has been derived from Schrodiner's LigPrep application module [LigPrep, Schrödinger, LLC, New York, NY, 2020] as a reference for future studies.

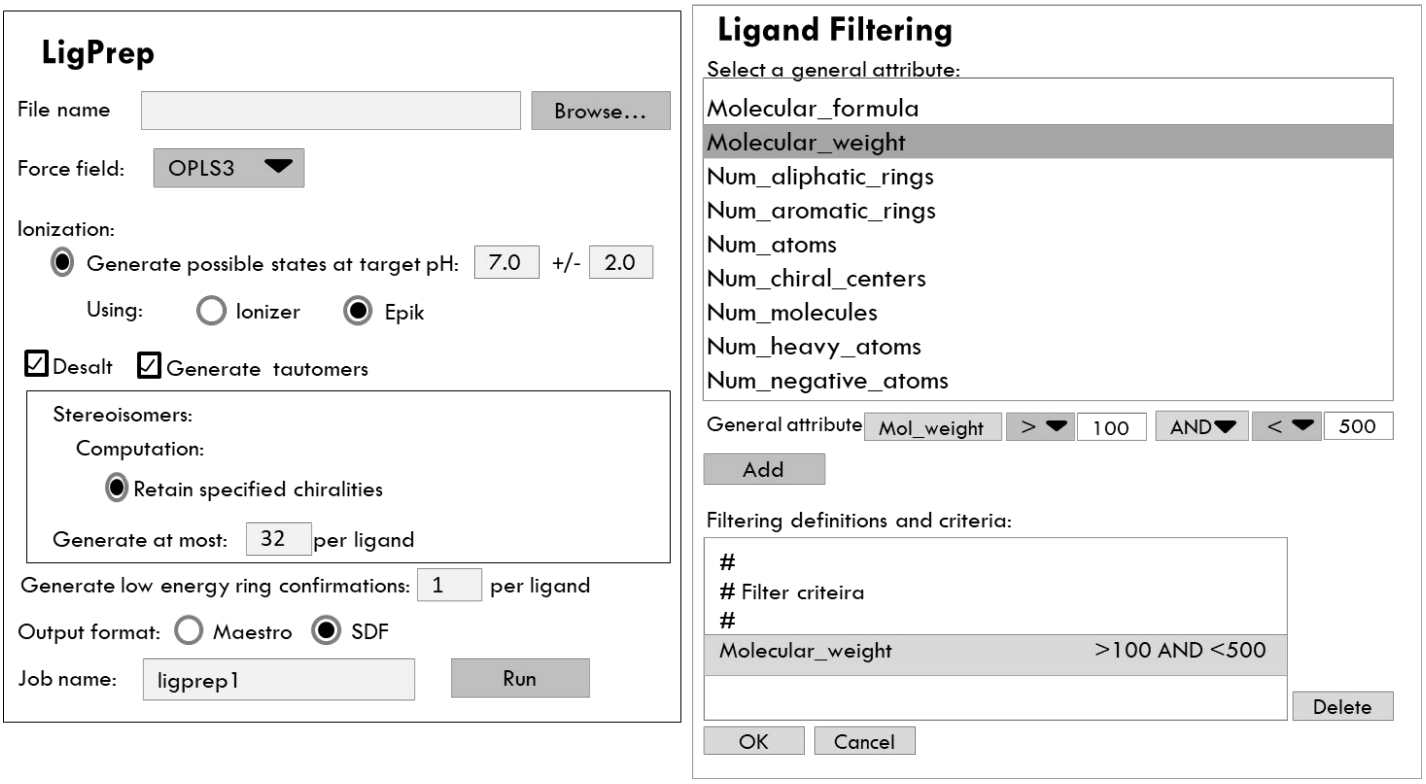

Figure S2: (A,B) The energy minimization of dimeric Hup model generated using YASARA homology modelling application. Energy minimization is performed using YASARA free webserver (http://www.yasara.org/minimizationserver.htm). The 94 amino acid sequence of *H. pylori* Hup derived from here: https://www.ncbi.nlm.nih.gov/protein/WP_001029082.1 (in FASTA format) is used as input for homology modeling (MNKAEFIDLV KEAGKYNSKR EAEEAISAFT LAVETALSKG ESVELIGFGK FETAEQKGKE GKVPGSDKTY KTEDKRVPKF KPGKTLKQKV EEGK). (C) The resulted dimeric Hup model was compared to those generated previously[2] using free web-based Protein Structure prediction server named (PS)2v2.[3,4] (D) The comparison has been made between energy minimized structures.

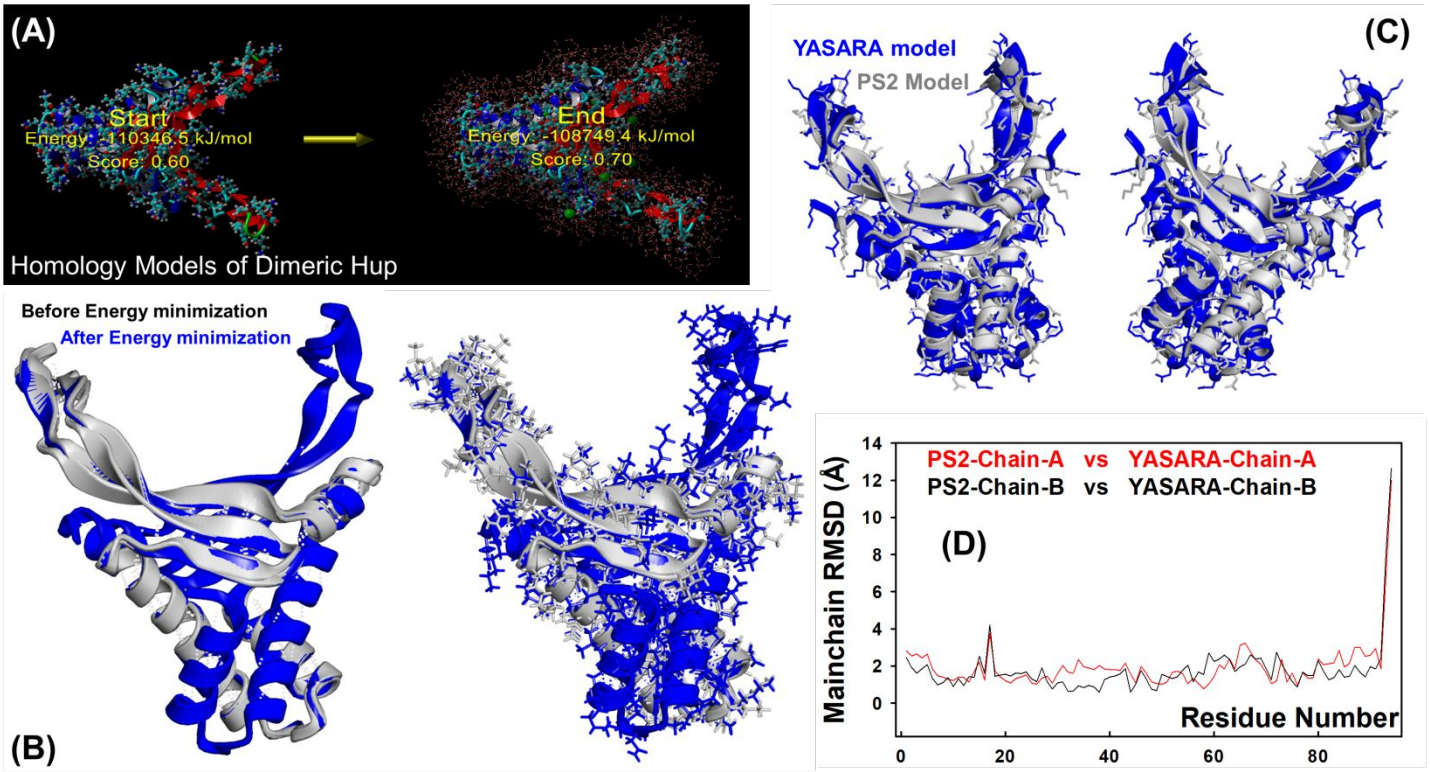

Figure S3: The energy minimization of monomeric Hup model performed using YASARA energy minimization webserver. The monomeric Hup structure has been extracted from Chain-B of homodimeric model generated using YASARA homology modelling.

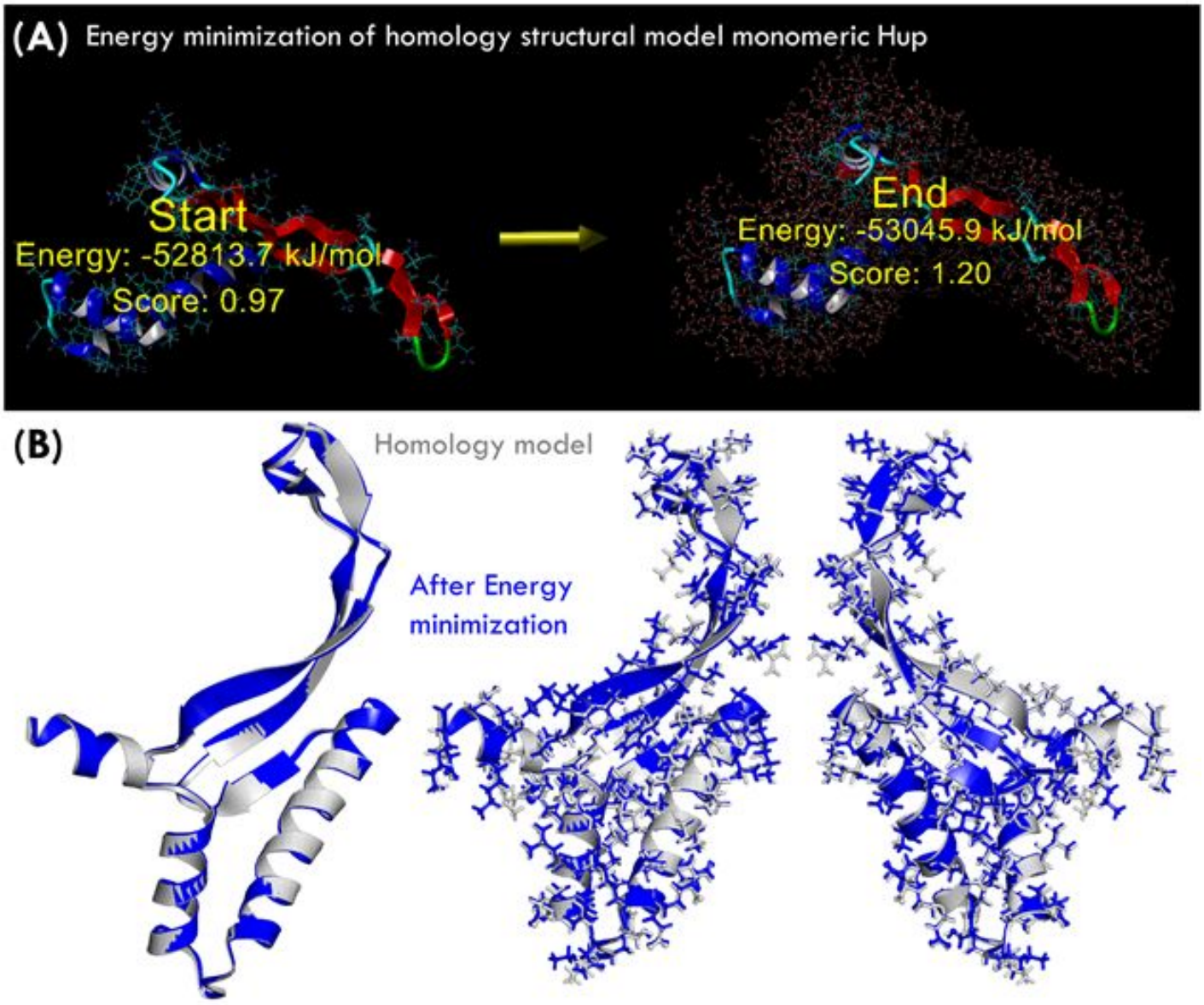

Appendix-I: Molecular Dynamics Simulations

Prior to simulation, the complex was cleaned and optimized for hydrogen bond network.[5] Next, a cubic simulation cell was created around the macromolecular system filled with water molecules and the periodic boundary condition was incorporated to perform the simulation. For charge neutrality as well as to mimic the biological conditions partly, the sodium and chloride (Na^+/Cl^-) ions were also added randomly to the system (by replacing the water molecules). The AMBER14 force field was employed to describe the macromolecular atoms in the simulation system.[6,7] The pKa values of titratable amino acids (e.g. Asp, Glu, His and Lys) were estimated and simulation box was solvated using the transferable intermolecular potential3 points (TIP3P) water model (density: 0.997 g/L) accordingly. Before MD simulation, each macromolecular system was energy minimized employing steepest descent approach (5000 cycles) followed by simulated annealing approach. All-atom MD simulations were performed employing particle-mesh Ewald (PME) method to describe long-range electrostatic interactions at a cut off distance of 8 Å and defining near physiological conditions at 298 K, pH 7.4 and 0.9% NaCl.[8] The simulation temperature was controlled using the Berendsen thermostat, where the pressure kept constant throughout the simulation. A multiple time step algorithm together with a simulation time step interval of 2.50 fs was chosen.[9] Long run MD simulations (more than 100 ns in each case) were performed at constant temperature using a Berendsen thermostat and constant pressure. MD trajectories were saved every 250 ps for further analysis. The MD trajectory data collected was analyzed using YASARA built in macro named "mdanalysis.mcr". The average structures were determined from the simulations and were used to calculate the Root-mean-square deviation (RMSD), root-mean-square fluctuation (RMSF), and number of H-bonds between solute and solvent for the respective macromolecular system. YASARA has a built-in protocol for calculating binding energies (BindEnergyObj command). The binding free energy ($\Delta G_{binding}$, referred here as binding energy) is obtained by calculating the energy at infinite distance between the selected object and the rest of the simulation system (i.e., the unbound state) and subtracting the energy of the simulation system (i.e., the bound state). As per the details provided in the YASARA manual, the free energy of an object is calculated without involving entropy term from normal mode analysis as.

$$G = E_{bind} + E_{el} + E_{vdw} + G_{polar} + G_{nonpolar} - TS \quad \text{(S1)}$$

Here, the first three terms are molecular mechanics (MM) terms of binding, electrostatic, and van der Waals interactions, respectively. Gpolar and Gnonpolar are polar and nonpolar contributions of solvation free energies, respectively. TS is the entropy effect, which is neglected when binding affinities are compared for the same ligand in different binding sites. Then binding free energy is calculated by the following equation:

$$\Delta G_{binding} = \left(G_{internal}^{Receptor} + G_{internal}^{Ligand}\right) + \left(G_{solvation}^{Receptor} + G_{solvation}^{Ligand}\right) - \left(G_{internal}^{complex} + G_{solvation}^{complex}\right) \text{ [kJ/mol]} \quad \text{(S2)}$$

Here, the first two terms are potential energies of the receptor and ligand, the next two terms are solvation energies of the receptor and ligand, and the last terms are potential and solvation energies of the complex. As mentioned in the help manual, YASARA sticks to standard convention and provides positive binding energies in KJ/mol. Note that more positive the binding energy, the more favorable the interaction in the context of the chosen force field, whereas negative energies indicates very weak binding, but DO NOT indicate no binding. Depending upon the system, more negative binding energy values indicate more favorable binding. For example, the negative binding energies (calculated using YASARA) has been reported previously for ligands binding to membrane-bound protein.[10] Relevant binding contacts between receptor and ligand were detected and visualized making composite use of YASARA software applications.

Table S1: The binding energy parameters derived from virtual screening of selected compound library against dimeric and monomeric Hup structures employing small molecule docking approaches (AUTODOCK, VINA and Glide). Natural compounds with highest cumulative binding energy were highlighted (with * mark and in Red color) for convenience.

ID	Autodock BE (Kcal/mol)		VINA BE (Kcal/mol)		Glide BE (Kcal/mol)		CBE (Kcal/mol)	Pubmed ID (CID)
	HupM	HupD	HupM	HupD	HupM	HupD		
1	6.93	7.32	6.74	6.58	3.50	0.58	5.27	2353
2	5.84	6.95	6.44	5.53	4.74	4.31	5.64	72300
3	6.35	7.56	6.58	5.51	4.42	0.00	5.07	72300
4	6.08	6.61	7.85	6.31	3.64	3.00	5.58	442126
5	5.15	6.04	4.66	5.05	4.49	5.15	5.09	370
6	5.75	6.17	5.10	5.29	2.38	2.14	4.47	444539
7	6.31	7.58	6.32	6.16	4.55	2.42	5.56	25201019
8	6.18	7.03	6.21	6.21	4.40	5.16	5.87	25201019
9	6.19	7.71	6.98	6.47	4.13	5.72	6.20	5281789
10	6.85	7.81	7.03	6.40	4.14	5.30	6.26	5281789
11	6.42	7.42	5.77	5.61	4.34	4.56	5.69	5281781
12	6.83	8.17	5.94	5.78	3.59	5.78	6.01	5281781
13	6.38	7.45	6.01	5.82	4.62	2.10	5.40	5280961
14	6.87	7.80	6.17	5.75	4.75	5.00	6.06	5280961
15	6.40	7.08	6.12	6.13	3.39	2.32	5.24	628528
16	6.37	7.24	6.23	6.24	4.22	3.44	5.62	72281
17	5.95	6.48	4.96	5.15	2.61	1.65	4.47	637542
18	6.54	6.89	4.99	5.14	3.54	4.27	5.23	689043
19	8.46	9.09	6.60	6.33	5.65	3.75	6.65	5281792
20	5.51	5.93	5.40	5.46	3.45	4.34	5.02	11644379
21	5.03	5.59	5.55	5.56	3.91	2.92	4.76	11218565

22	5.32	5.99		5.37	4.93		2.79	1.56		4.33	11218565
23	6.00	6.26		5.60	5.44		4.18	0.00		4.58	6857681
24	5.32	6.35		5.43	4.55		2.95	0.00		4.10	15560069
25	6.98	8.75		8.91	8.04		3.49	5.12		6.88	10114
26	5.01	5.11		4.04	4.40		3.40	5.04		4.50	1183
27	5.23	5.63		4.31	4.19		2.82	3.69		4.31	1183
28	6.72	7.51		7.10	6.03		4.22	4.22		5.97	14287147
29	6.54	7.76		7.18	6.56		3.29	3.48		5.80	14680349
30	7.44	7.78		7.33	5.94		4.40	2.40		5.88	101297697
31	5.72	6.61		5.15	5.35		3.96	2.83		4.94	44584263
32	6.32	7.17		5.59	5.63		3.96	0.28		4.82	44584263
33	6.43	7.39		6.06	5.94		3.48	3.93		5.54	5352001
34	7.19	7.59		6.06	6.05		3.79	5.26		5.99	5352001
35	6.32	6.83		6.04	6.12		4.58	2.53		5.40	5459196
36	7.03	7.58		5.95	6.27		4.01	2.72		5.59	5459196
37	6.17	7.30		6.01	6.08		3.91	5.02		5.75	5281666
38	6.97	7.77		6.07	6.29		4.84	6.94		6.48	5281666
39	4.92	5.57		4.95	4.68		3.16	2.03		4.22	7444
40	4.71	6.98		5.11	4.23		4.11	0.00		4.19	167551
41	6.50	7.89		6.25	6.05		3.81	3.01		5.58	443023
42	5.67	5.72		4.92	5.14		3.67	2.48		4.60	3806
43	6.28	6.52		4.93	5.06		2.77	0.26		4.30	3806
44	6.59	7.90		6.07	5.86		3.91	3.25		5.60	92503
45	6.54	7.78		6.03	5.98		3.12	6.63		6.01	92503
46	6.01	7.02		6.37	6.00		3.85	7.64		6.15	5319013
47	6.23	7.88		6.46	6.20		4.01	7.37		6.36	5319013
48	6.35	6.31		6.82	6.41		4.84	2.60		5.56	480873
49	6.53	7.62		6.90	6.69		3.07	3.33		5.69	480865
50	6.37	7.32		6.56	6.16		4.08	3.24		5.62	114829
51	6.55	8.05		7.19	6.70		4.23	5.79		6.42	124052
52	7.02	7.62		7.26	7.18		4.60	3.84		6.25	480774
53	6.79	7.27		6.82	6.44		3.38	4.78		5.91	5320083
54	7.43	8.29		6.96	6.75		3.74	4.76		6.32	5320083
55	6.97	9.14		6.29	6.06		5.72	1.42		5.93	1794427
56	6.79	7.37		6.20	6.21		3.79	2.95		5.55	440735
57	6.74	7.47		6.06	6.28		5.22	3.30		5.84	439533
58	7.38	8.48		6.01	6.42		4.46	4.64		6.23	439533
59	6.60	7.87		5.89	6.18		6.01	3.00		5.92	5281691
60	7.44	8.48		6.10	6.29		4.76	4.91		6.33	5281691
61	6.35	6.72		6.06	5.96		4.18	1.89		5.19	6442633
62	6.06	6.06		6.15	5.88		4.13	3.18		5.24	6442633
63	6.90	6.89		6.25	6.01		4.10	2.71		5.48	6442633

64	6.31	6.55		6.24	5.74		3.17	3.99		5.33	6442633
65	6.78	7.41		6.16	5.80		4.09	3.88		5.69	6442633
66	6.39	6.53		6.11	6.00		4.01	3.80		5.47	6442633
67	6.66	7.28		5.95	6.13		3.99	3.79		5.63	6442633
68	6.47	7.00		5.93	5.80		3.98	3.62		5.47	6442633
69	6.82	7.06		6.14	5.67		3.97	3.54		5.53	6442633
70	6.30	6.96		6.06	5.68		3.93	0.79		4.95	6442633
71	5.94	6.67		6.37	5.98		3.92	3.48		5.39	6442633
72	6.40	6.82		6.15	6.64		3.91	3.46		5.56	6442633
73	7.05	6.86		6.00	5.93		3.91	3.44		5.53	6442633
74	6.32	6.86		6.05	5.84		3.88	3.39		5.39	6442633
75	7.06	7.14		6.38	6.32		3.85	3.36		5.69	6442633
76	6.94	6.86		6.02	6.39		3.84	3.36		5.57	6442633
77	6.13	6.29		6.15	5.79		3.83	3.28		5.24	6442633
78	6.28	7.16		6.44	6.19		3.82	3.22		5.52	6442633
79	7.04	6.93		6.15	6.21		3.80	3.20		5.56	6442633
80	6.70	6.39		6.09	6.35		3.78	4.25		5.59	6442633
81	6.86	6.99		5.99	6.02		3.78	3.18		5.47	6442633
82	6.29	7.05		6.22	6.19		3.70	3.17		5.44	6442633
83	6.50	7.52		6.14	5.87		3.58	3.16		5.46	6442633
84	6.66	7.61		6.11	6.23		3.58	3.07		5.54	6442633
85	6.39	7.36		6.29	5.97		3.57	2.97		5.43	6442633
86	6.39	6.20		6.32	5.70		3.55	2.94		5.18	6442633
87	5.90	7.04		5.83	6.09		3.55	2.90		5.22	6442633
88	6.81	6.83		6.59	6.34		3.54	2.87		5.50	6442633
89	6.33	6.82		6.02	5.96		3.53	2.72		5.23	6442633
90	6.46	6.56		6.31	5.85		3.49	4.12		5.46	6442633
91	6.52	6.50		6.41	6.20		3.40	2.65		5.28	6442633
92	7.09	6.78		6.05	6.03		3.33	1.54		5.14	6442633
93	7.32	6.92		6.37	6.04		3.40	7.51		6.26	7605278
94	5.87	7.05		6.05	5.78		4.10	5.15		5.67	445154
95	7.37	7.87		6.28	6.76		5.38	-3.00		5.11	65064
96*	8.47	8.91		6.43	6.63		5.46	8.33		7.37	65064
97	8.33	8.99		6.39	7.24		5.81	7.28		7.34	65064
98	4.96	6.24		5.43	5.07		2.40	0.00		4.02	5281794
99	7.16	7.80		6.16	6.20		5.28	3.29		5.98	5281855
100	8.14	8.79		6.32	6.38		4.89	5.81		6.72	5281855
101	8.20	8.85		6.39	6.38		4.85	2.49		6.19	5281855
102	6.73	7.83		6.07	6.09		5.55	5.11		6.23	5281672
103	7.51	8.75		5.92	6.24		5.29	4.79		6.42	5281672
104	6.58	7.72		6.93	6.98		4.36	10.02		7.10	969516
105	6.37	7.93		6.88	6.85		5.33	3.80		6.19	969516

106	6.56	8.15		6.67	6.67		5.14	3.76		6.16	969516
107	6.43	8.17		6.70	6.40		4.78	2.32		5.80	969516
108	6.50	7.92		6.70	6.33		4.03	0.93		5.40	969516
109	4.37	4.65		5.41	4.48		3.20	5.34		4.58	358901
110	4.83	5.16		4.21	4.16		2.50	3.46		4.05	243
111	4.17	4.39		3.79	4.65		3.70	2.38		3.85	289
112	3.78	4.22		3.35	3.25		2.16	1.48		3.04	5350
113	3.66	4.14		3.22	3.40		2.11	4.50		3.50	5350
114	1.73	3.98		4.14	4.30		4.31	6.52		4.16	6251
115	2.27	2.85		1.90	2.97		1.74	0.00		1.96	6344
116	4.16	4.17		5.02	4.56		3.45	3.02		4.06	6989
117	4.78	5.89		4.60	5.14		3.98	5.74		5.02	7428
118	5.52	6.19		4.71	5.02		3.43	3.57		4.74	7428
119	5.59	6.86		4.68	5.03		3.59	3.37		4.85	7428
120	4.26	5.05		5.04	4.55		3.21	0.00		3.68	7461
121	3.99	4.87		5.08	4.56		3.07	0.00		3.59	7463
122	4.51	4.49		5.01	4.93		3.75	2.00		4.12	10364
123	5.49	5.78		4.13	4.55		3.23	3.55		4.46	10742
124	4.18	4.84		4.52	4.50		3.66	5.68		4.56	11092
125	4.92	5.60		4.49	4.58		2.77	1.55		3.98	11092
126	4.57	4.80		5.04	4.92		2.63	1.53		3.92	17100
127	4.52	4.83		4.90	4.81		2.60	2.00		3.94	17100
128	4.43	4.56		4.95	4.60		2.43	1.88		3.81	61041
129	3.88	4.67		3.30	3.25		1.87	0.83		2.97	65036
130	3.71	4.79		3.37	3.14		1.45	5.78		3.71	65036
131	4.11	4.84		4.07	4.21		3.63	4.50		4.23	69600
132	4.92	5.50		4.04	4.32		2.50	1.04		3.72	69600
133	6.33	7.04		5.99	6.50		3.30	2.72		5.31	10333023
134	7.45	7.25		6.48	6.17		3.97	2.12		5.57	73174
135	6.69	7.10		6.36	6.54		3.34	2.21		5.37	73440
136	6.62	7.33		6.97	5.91		3.48	6.21		6.09	73440
137	6.96	7.47		5.17	5.11		3.35	3.94		5.33	83043
138	6.14	8.18		6.18	6.73		5.42	4.19		6.14	162350
139	7.18	9.70		6.17	6.86		4.54	1.19		5.94	162350
140	5.07	5.92		4.96	5.13		4.08	4.19		4.89	168114
141	4.55	5.88		5.38	4.80		4.63	2.23		4.58	168115
142	7.81	9.66		8.04	7.14		4.30	3.98		6.82	265237
143*	8.87	10.39		8.22	7.50		3.48	5.61		7.34	265237
144	4.70	5.72		4.53	4.93		4.06	2.59		4.42	287064
145	5.20	6.29		4.67	4.95		3.38	4.21		4.78	287064
146	6.58	6.70		6.10	5.79		4.25	2.21		5.27	336327
147	6.35	6.90		5.51	5.95		4.98	5.53		5.87	439514

148	6.66	7.13		6.10	5.91		3.46	5.60		5.81	10333024
149	4.73	6.41		4.51	5.23		3.01	3.79		4.61	442793
150	6.46	6.95		6.81	5.81		3.67	2.23		5.32	101401747
151	6.13	6.56		4.97	5.12		3.51	2.97		4.88	445858
152	4.95	5.07		4.62	4.61		2.62	1.11		3.83	637776
153	7.45	8.27		6.90	6.27		3.29	5.84		6.34	638024
154	5.97	7.05		6.30	6.29		5.52	4.12		5.87	5280441
155	6.56	7.79		6.51	6.45		5.42	4.29		6.17	5280441
156	6.87	7.28		8.77	6.74		3.52	4.82		6.33	42607682
157*	7.60	9.15		9.40	7.57		3.41	6.02		7.19	42607682
158	6.40	7.29		6.48	6.17		4.67	4.04		5.84	5280443
159	7.30	8.07		6.53	6.32		4.79	6.03		6.51	5280443
160	6.54	7.47		6.33	6.14		5.31	6.63		6.40	5280445
161*	7.67	8.43		6.38	6.29		5.21	8.79		7.13	5280445
162	7.93	7.69		6.26	6.43		4.39	3.64		6.06	5280459
163	8.44	8.61		6.24	6.62		5.28	5.35		6.76	5280459
164	5.61	6.46		4.98	5.07		3.36	3.84		4.89	5280460
165	6.36	6.64		4.96	5.06		3.06	5.22		5.22	5280460
166	6.39	7.53		6.27	6.32		4.76	3.93		5.87	5281605
167	6.83	8.04		6.31	6.48		4.49	4.86		6.17	5281605
168	6.27	6.82		6.77	6.55		4.30	3.73		5.74	5281650
169	6.54	7.76		6.89	6.62		4.75	4.95		6.25	5281650
170	6.83	7.86		6.78	6.54		3.73	5.30		6.17	5281650
171	6.58	7.02		5.83	5.89		4.32	3.91		5.59	5281811
172	6.92	7.72		5.99	5.81		3.95	2.88		5.55	5281811
173	5.72	6.16		5.69	5.83		3.22	4.38		5.17	5281832
174	6.62	6.73		5.84	6.07		3.23	5.97		5.74	5281832
175	6.00	6.79		6.90	5.93		4.60	3.78		5.67	5318998
176	6.66	7.63		6.92	6.26		3.00	4.60		5.85	5318998
177	6.99	7.20		5.59	6.07		5.08	2.65		5.60	5319518
178	7.67	8.06		5.96	6.33		3.94	6.64		6.43	5319518
179	7.30	8.04		5.76	6.24		5.15	5.12		6.27	5319518
180	7.69	7.96		5.71	6.19		4.80	5.03		6.23	5319518
181	6.74	7.07		5.56	5.84		4.65	6.96		6.14	5319518
182	7.41	8.01		5.70	5.95		4.60	5.26		6.16	5319518
183	7.20	7.55		5.69	5.80		4.83	5.92		6.17	5319518
184	7.17	7.56		5.70	5.99		2.20	4.55		5.53	5319518
185	6.33	7.18		6.26	5.97		5.19	3.91		5.81	5320946
186	7.15	8.13		6.43	6.16		3.99	1.35		5.53	5320946
187	5.01	5.23		6.26	5.46		3.64	4.39		5.00	5470187
188	6.09	6.67		6.67	6.45		4.50	7.71		6.35	5495925
189	6.04	7.73		6.82	6.53		2.56	2.95		5.44	5495925

190	7.93	8.66		6.51	6.69		5.92	4.35		6.68	6419835
191*	8.76	8.82		6.65	6.64		5.57	7.19		7.27	6419835
192	8.74	9.52		6.62	6.82		4.04	3.50		6.54	6419835
193	7.77	7.86		7.60	7.11		3.18	3.00		6.09	6451060
194	5.85	7.19		4.76	4.99		6.29	3.85		5.49	9548634
195	5.01	7.06		4.76	5.29		6.24	4.51		5.48	9548634
196	7.80	8.60		6.57	6.75		4.88	2.82		6.24	10095770
197	5.71	7.61		6.74	6.74		3.17	2.89		5.48	10386850
198	6.74	8.51		6.86	6.90		4.17	4.94		6.35	10386850
199	7.38	8.82		6.86	6.89		4.10	2.78		6.14	10386850
200	5.64	5.66		6.44	5.45		3.62	6.67		5.58	10955174
201	5.29	6.03		5.75	5.99		3.50	1.62		4.70	11165077
202	5.95	5.76		5.66	5.34		4.11	2.54		4.89	11223782
203	4.97	5.67		5.65	5.90		3.33	5.93		5.24	11673265
204	5.77	5.95		6.80	5.83		4.44	4.57		5.56	11827150
205	6.22	7.26		6.52	6.59		5.29	4.52		6.07	11827150
206	5.35	8.41		6.45	5.97		3.98	2.25		5.40	11827150
207	4.96	6.23		5.71	5.70		4.46	3.09		5.02	16091559
208	5.83	6.48		6.49	6.24		5.19	4.45		5.78	44258361
209	5.48	6.42		6.43	6.01		5.17	4.56		5.68	44258361
210	5.40	6.44		6.44	6.30		5.03	3.87		5.58	44258361
211	5.30	6.28		6.55	6.25		4.73	4.32		5.57	44258361
212	7.18	8.13		8.59	7.32		5.63	5.56		7.07	44421210
213	7.28	7.93		8.70	6.72		5.33	4.28		6.71	44421210
214	8.39	8.61		8.45	7.19		4.17	3.56		6.73	44421210
215	7.75	8.23		8.57	6.80		3.63	3.27		6.37	44421210
216	7.06	8.18		8.22	7.10		3.72	2.55		6.14	52947057
217	6.68	8.33		8.19	6.48		3.56	4.16		6.23	52947057
218	5.26	5.38		5.05	4.84		3.47	6.13		5.02	62379750
219	5.83	5.98		5.33	4.90		3.56	5.24		5.14	62379750
220	4.43	5.09		5.01	5.12		3.39	4.91		4.66	92023653
221	6.68	7.27		5.98	5.91		4.13	4.14		5.69	101918993
222	7.10	7.62		7.76	7.30		3.26	2.69		5.95	4970
223	7.16	7.73		8.06	7.20		2.94	-1.20		5.32	4970
224	7.81	8.52		7.86	7.26		3.10	5.51		6.68	4970
225	3.89	4.28		3.38	3.39		2.33	1.85		3.19	11620
226	4.02	4.58		3.20	3.57		2.33	1.48		3.20	11620
227	3.90	4.32		3.15	3.46		2.32	1.14		3.05	11620
228	4.14	4.63		3.29	3.48		2.30	3.35		3.53	11620
229	5.83	5.73		4.98	5.17		3.27	2.74		4.62	16871
230	6.41	7.56		5.85	5.68		3.48	2.58		5.26	10682896
231	3.26	3.76		2.63	2.78		1.76	6.59		3.46	78160

232	6.17	6.74		6.83	6.73		4.02	1.08		5.26	179806
233	5.94	7.27		7.22	6.80		3.82	1.64		5.45	197835
234	6.74	7.73		7.10	6.46		3.12	-0.26		5.15	197835
235	7.78	7.92		6.78	6.73		3.50	1.46		5.69	197835
236	3.81	4.68		3.40	3.61		2.33	0.50		3.05	206035
237	3.95	4.19		3.45	3.60		1.91	2.92		3.34	206035
238	3.38	3.79		3.07	3.10		2.03	2.95		3.05	206037
239	6.33	6.55		6.70	6.09		3.51	3.96		5.52	442361
240	3.67	4.25		3.48	3.56		2.33	7.78		4.18	3080557
241	6.70	8.07		8.32	6.81		3.21	3.80		6.15	5281331
242	5.30	6.26		5.38	4.68		3.11	0.00		4.12	5317303
243	4.53	6.28		5.35	4.72		2.87	2.99		4.46	5319779
244	6.27	6.50		5.94	6.19		3.65	5.31		5.64	14466152
245	5.80	6.86		6.17	5.35		4.50	5.17		5.64	11848147
246	6.10	6.42		6.65	5.97		3.97	6.06		5.86	11848147

Note: The virtual screening in Schrödinger was conducted using Glide (10.5) module which invokes ChemScore empirical scoring function.

$$\Delta G_{binding} = \Delta G_{match} F_{match} + \Delta G_{lipo} F_{lipo} + \Delta G_{ambig} F_{ambig} + \Delta G_{clash} F_{clash} + \Delta G_{rot} n_{rot}$$

ΔG_i *are coefficients and* F_i *are functions*

ΔG_{match} is a sum of scores for directed interactions between receptor and ligand.

The terms F_{match} provide a measure of hydrophobic contact surface as functions of atomic pairs in receptor and ligands, F_{lipo} involving only pairs of unpolar atoms and F_{ambig} involving pairs of one polar and one unpolar atom. Finally, F_{clash} is a penalty function for protein ligand overlap, and n_{rot} is equal to the number of rotatable bonds in the ligand times a weighting factor by default is set as 1. The term $\Delta G_{rot} n_{rot}$ was originally intended as a measure of the entropic cost of freezing intramolecular degrees of freedom in the ligand upon binding with receptor. Virtual screening, mainly serves to suppress the dependence of the score on the molecular weight.[11]

The natural compound database was subjected to screening based on extra precision (XP) docking against minimized conformations of Hup receptor created grid.[12]

$$XP\ Glide\ Score = E_{coul} + E_{vdW} + E_{bind} + E_{penality}$$

$$E_{bind} = E_{hyd-enclosure} + E_{hb-nn-motif} + E_{hb-cc-motif} + E_{PI} + E_{hb-pair} + E_{phobic-pair}$$

$$E_{penality} = E_{desovation} + E_{ligand\_strain}$$

$E_{hyd-enclosure}$ Represents Hydrophobic Interaction, E_{hb} represents hydrogen bonds.

All 246 molecular structures were subjected to Induced-fit standard precision docking in which hydroxyl groups are allowed to reorient thus allowing hydrogen bonding. For each ligand 400 poses we generated and van der Waals scaling of 0.4 Å was allocated on non-polar atoms of both protein and ligand. Keeping prime energy values within 20 kcal/mol, the ligands were re-docked on prime refined structure whereby minimizing the docked pose within the radius of 5 Å.[13]

Figure S4: Long run MD-simulation performed in explicit water solvent for ligand free and bound forms of monomeric Hup (HupM) and dimeric Hup (HupD). (A) A representative ray-traced picture of simulated system with simulation cell boundaries set to periodic. Atoms that stick out of the simulation cell will be wrapped to the opposite side of the cell during the simulation. (B) The table showing components of the system and time of simulation. (C, D) The backbone conformations of ligand free HupD and HupM structures compared before and after the MD simulation. (E-G) The docked conformations of Hup-EGCG complex compared before and after the long run MD simulations.

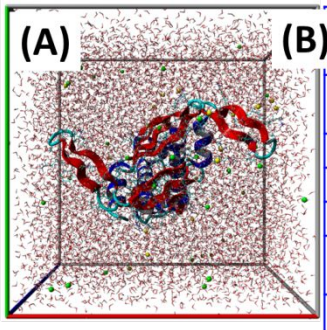

Composition of the system	Free Hup		ECGC in complex with		
	HupD	HupM	HupD	HupM-1	HupM-2
Protein molecules	2	1	2	1	1
Protein residues	188	94	188	94	94
Protein atoms	2972	1486	2972	1486	1486
Water residues	10098	11903	10463	11889	11889
Total number of atoms	33322	37262	34470	37269	37269
Simulation time (ns)	301	258	281	253	285

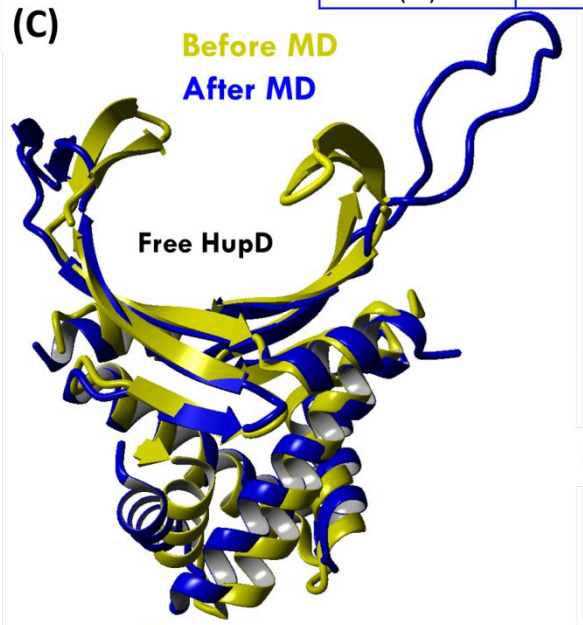

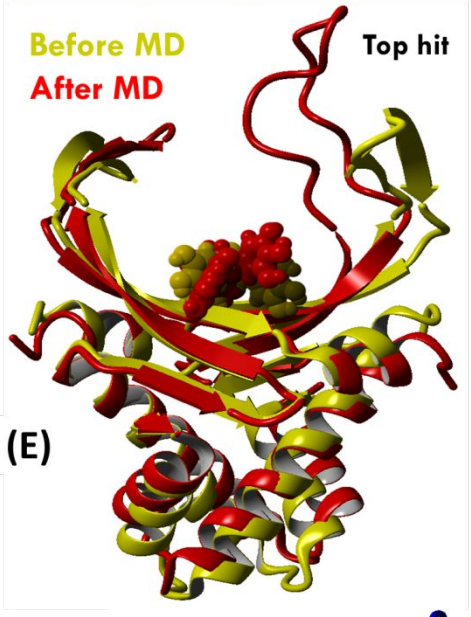

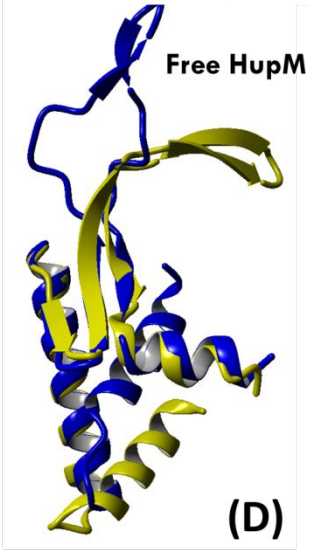

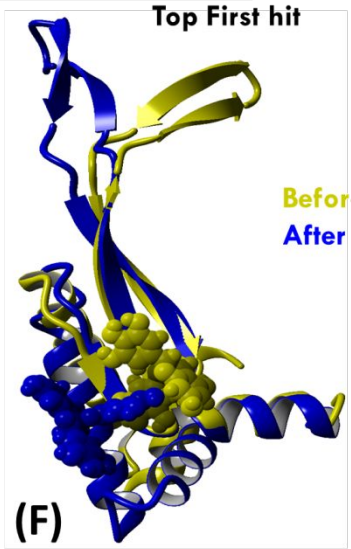

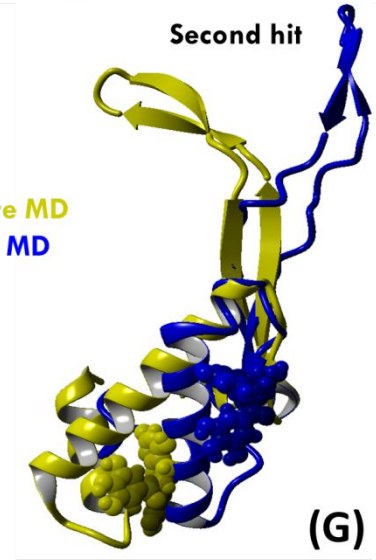

Figure S5: The trajectory analysis of MD-simulation data (on free Hup) performed in three blocks. The plots in (A, B and C) and (A', B' and C') show the results, respectively, on HupD and HupM: (A,A') total potential energy of the system, (B,B') number of hydrogen bonds between solute and solvent and (C,C') protein secondary structure content as a function of simulation time.

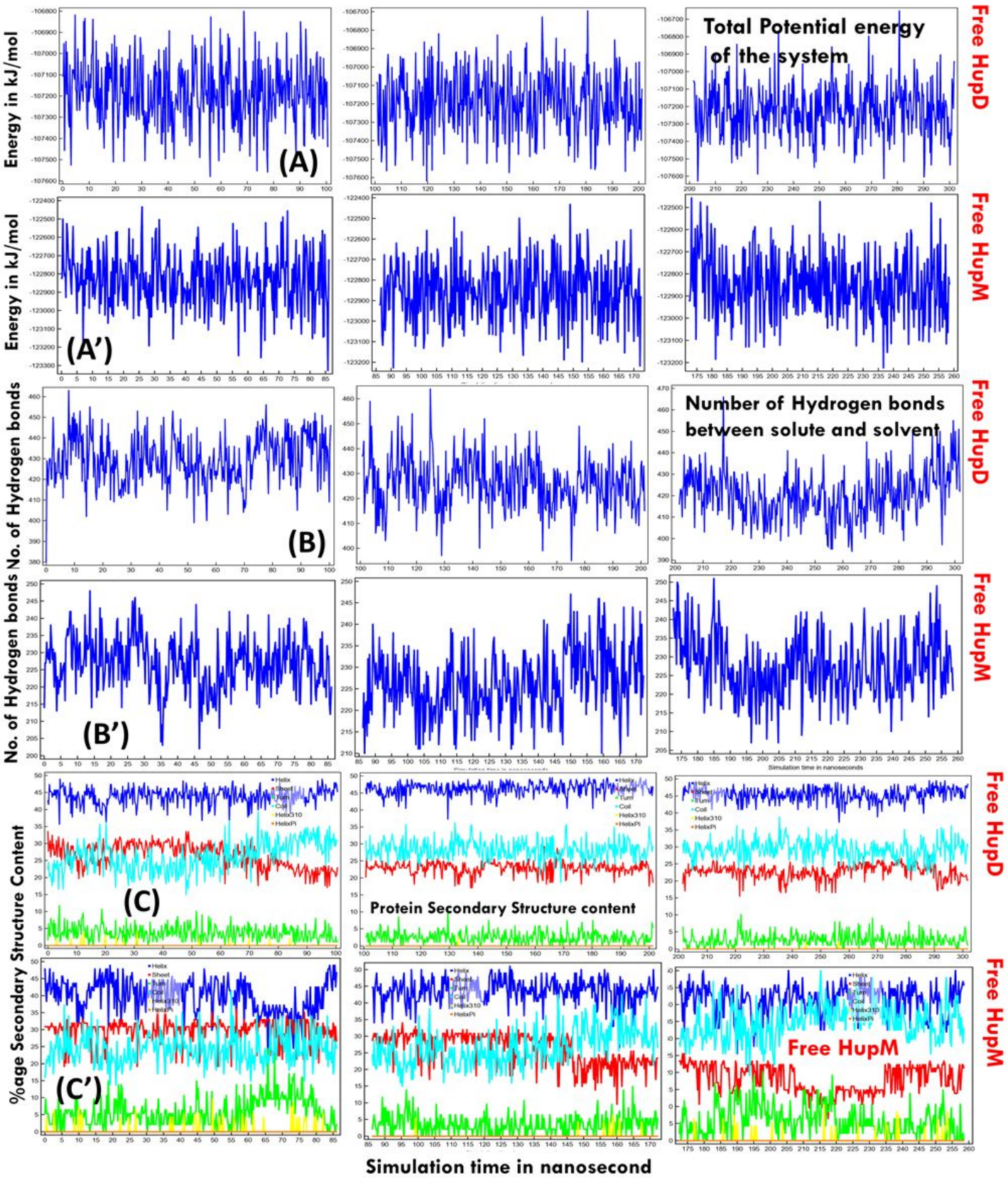

Figure S6: The trajectory analysis of MD-simulation data (on free Hup) performed in three blocks. The plots in (A, B and C) and (A', B' and C') show the results, respectively, on HupD and HupM: (A,A') Radius of

gyration of protein in angstrom (Å), (B,B') backbone Root mean square deviation (RMSD) (C,C') Root mean square fluctuations (RMSF) during the simulation plotted as a function of residue number.

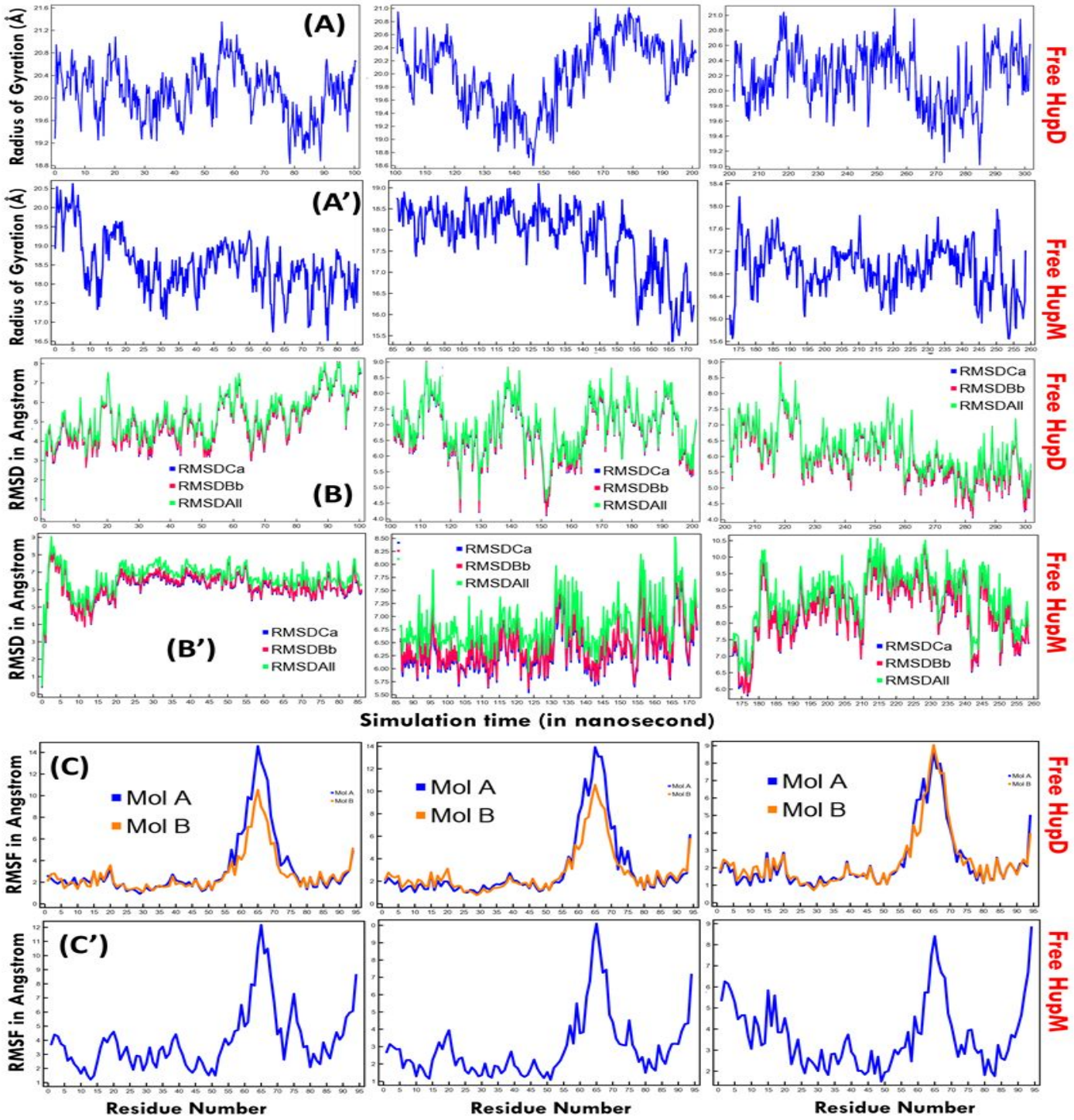

Figure S7: (A,B) Time evolution of protein residue secondary structure type during the MD simulation on free Hup (trajectory analysis was performed in three blocks) (C,D) The time evolution of number of contacts per residue as to see how densely a certain residue range is packed and allows identifying structurally very important residues, e.g. a phenylalanine in the hydrophobic core can contact 15 or more other residues.

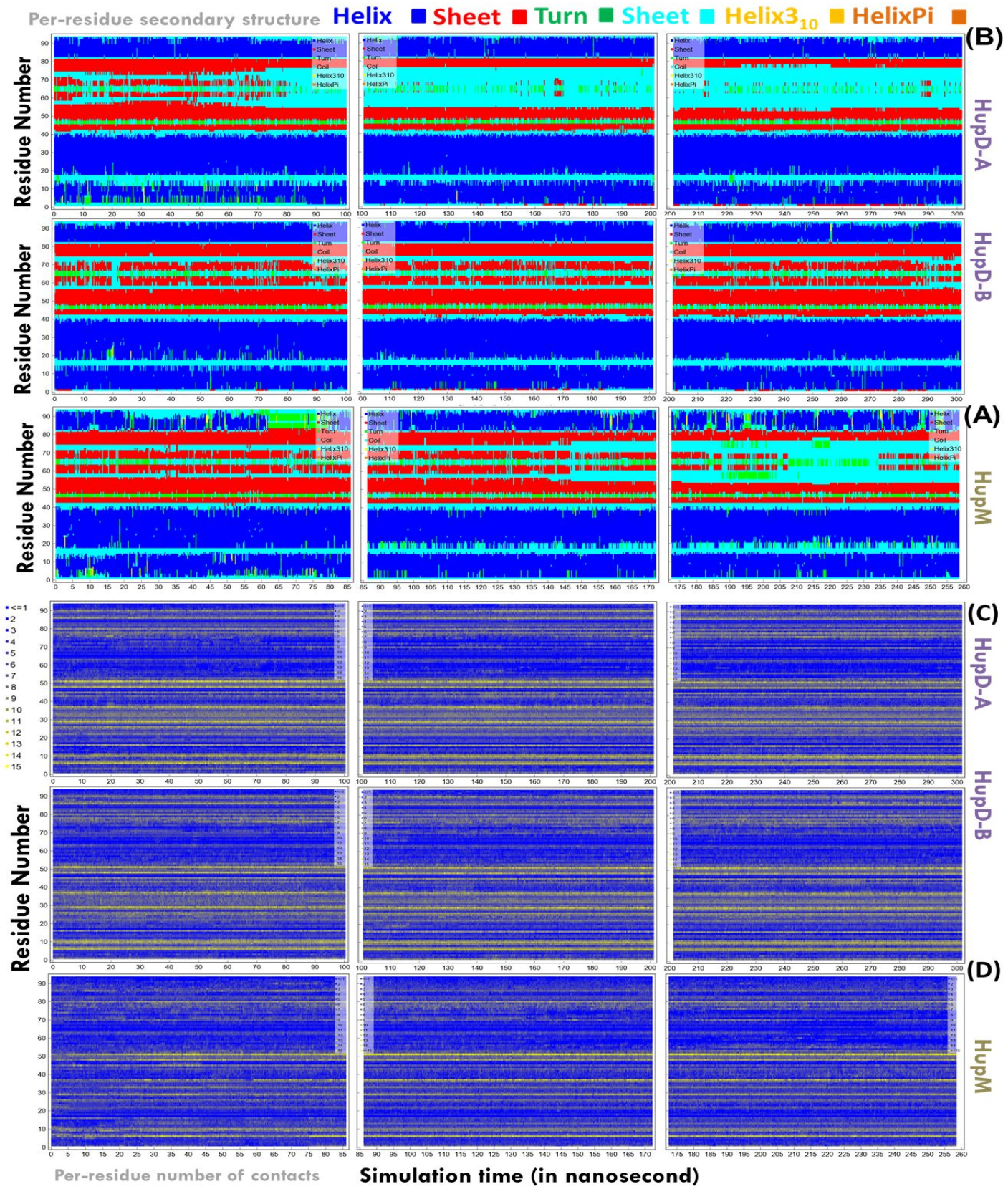
Per-residue secondary structure Helix Sheet Turn Sheet Helix3$_{10}$ HelixPi
(B)
HupD-A
HupD-B
(A)
HupM
(C)
HupD-A
HupD-B
(D)
HupM
Residue Number
Helix
Sheet
Turn
Coil
Helix310
HelixPi
<=1
2
3
4
5
6
7
8
9
10
11
12
13
14
15
Per-residue number of contacts
Simulation time (in nanosecond)

Figure S8: The results obtained from the trajectory analysis of MD simulation data on top two best complexes of EGCG with HupM. (A,A') Total potential energy of the system plotted as a function of simulation time. (B, B') The plot shows the number of hydrogen bonds between solute and solvent as a function of simulation time. (C,C') The plot shows time evolution of protein secondary structure content.

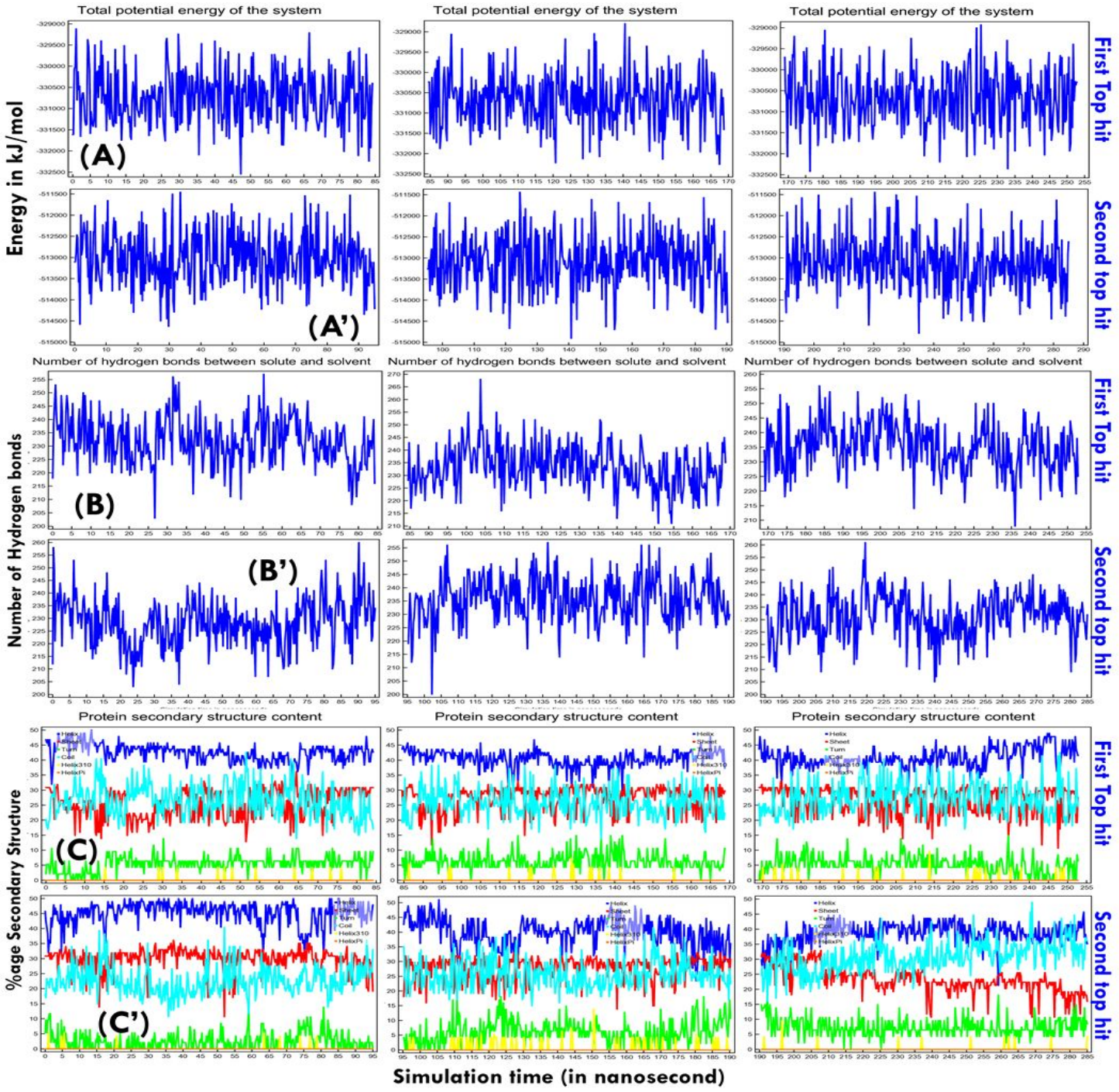

Figure S9: The results obtained from the trajectory analysis of MD simulation data on top two best complexes of EGCG with HupM. (A,A') Radius of gyration plotted as a function of simulation time. (B, B') Protein RMSD from the starting structure plotted as a function of simulation time. (C,C') The protein residue-wise root mean square fluctuation (RMSF) calculated from the average RMSF of the atoms constituting the residue.

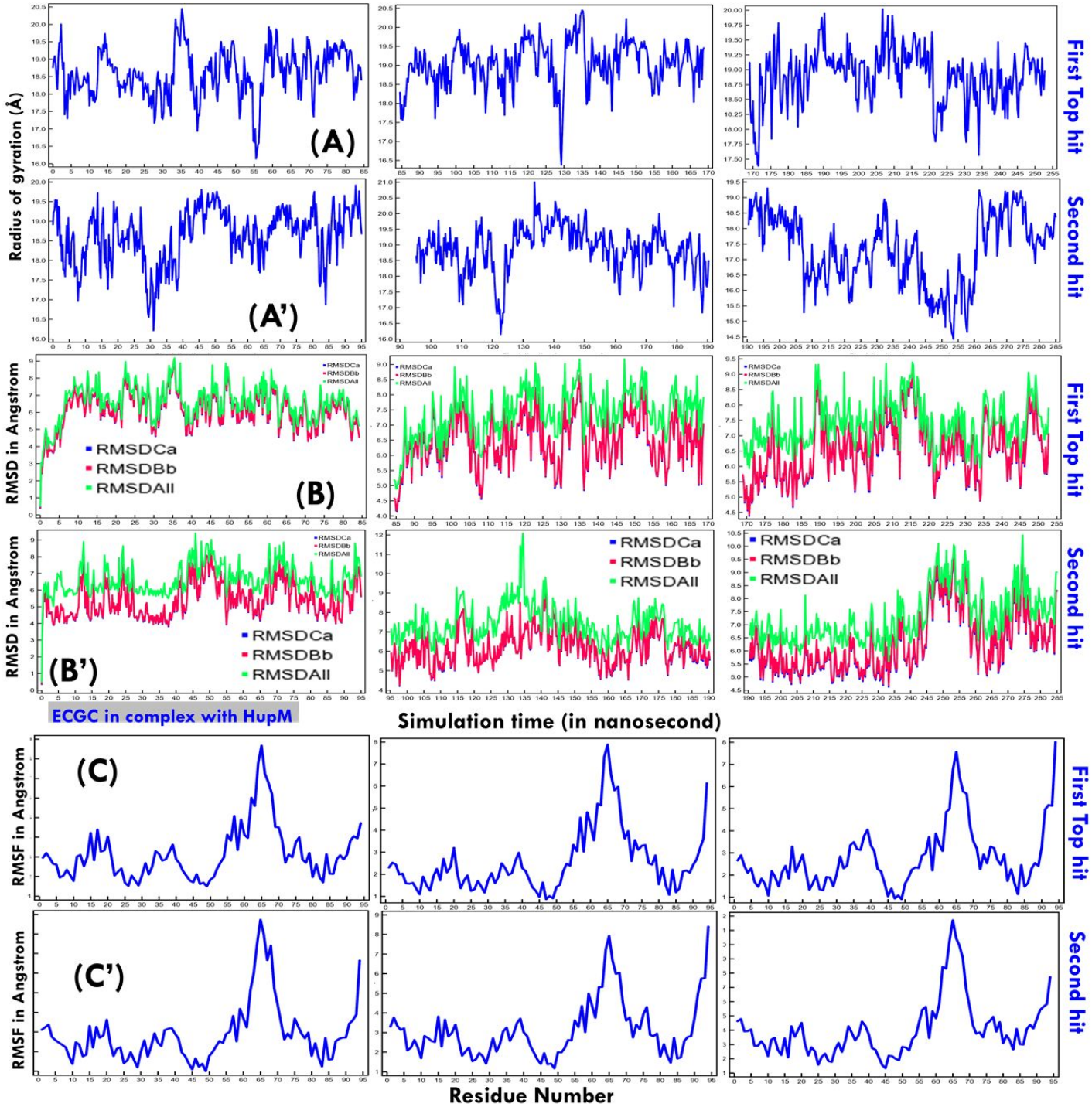

Figure S10: The results obtained from the trajectory analysis of MD simulation data on top two best complexes of EGCG with HupM. (A,A') The ligand movement RMSD measured after superposing the receptor on its reference structure. This procedure delivers information about the movement of the ligand in its binding pocket. (B, B') The ligand conformation RMSD after superposing on the ligand plotted as a function of simulation time. This provides information about the conformational changes of the ligand. (C,C') The time evolution of number of contacts per residue as to see how densely a certain residue range is packed and allows identifying structurally very important residues, e.g. a phenylalanine in the hydrophobic core can contact 15 or more other residues.

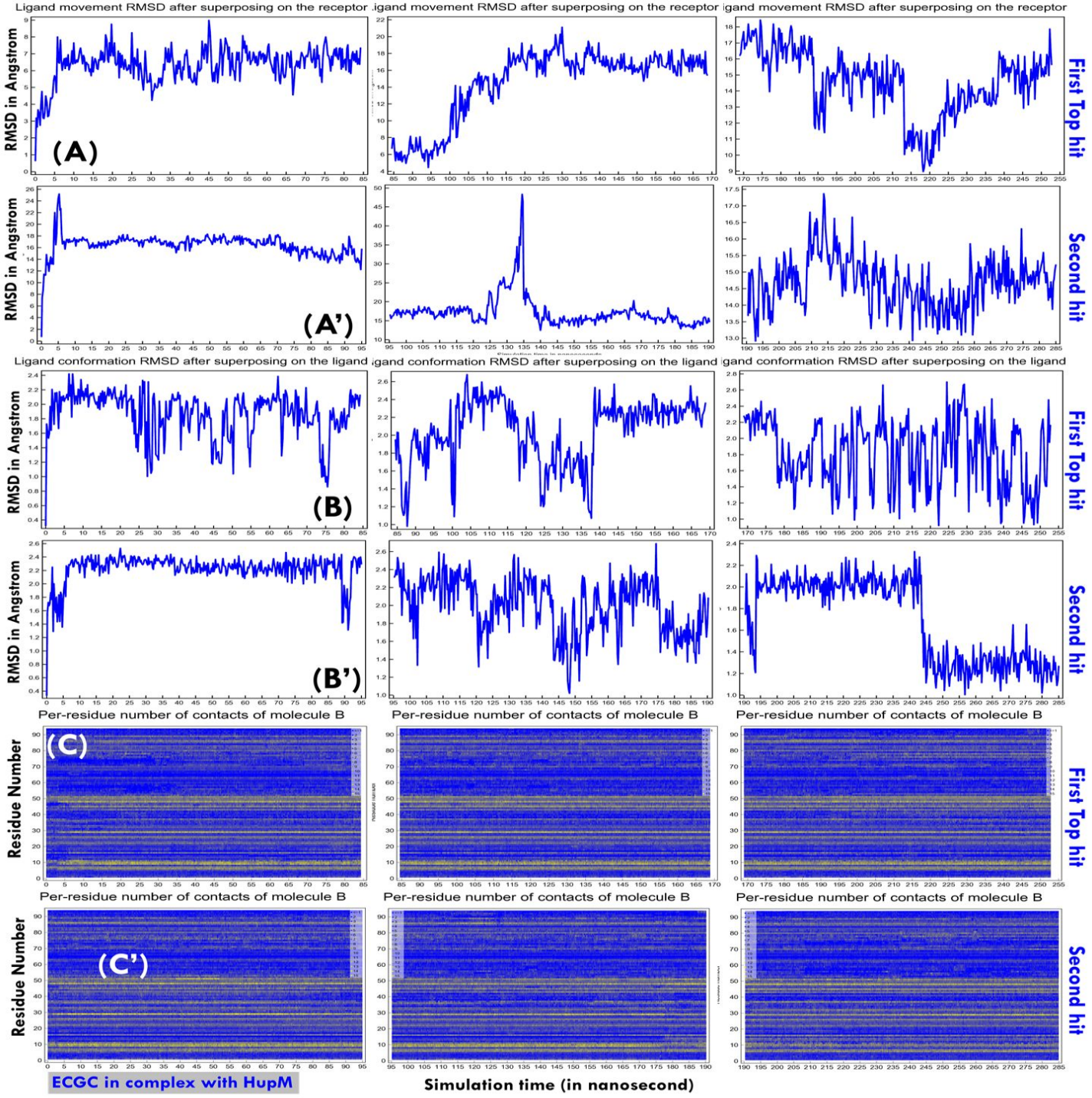

Figure S11: The results obtained from the trajectory analysis of long run MD simulation data on EGCG-HupD complex with highest binding energy. (A) Total potential energy of the system plotted as a function of simulation time. (B) The plot shows the number of hydrogen bonds between solute and solvent as a function of simulation time. (C) The plot shows protein secondary structure content as a function of simulation time. (D) The ligand movement RMSD measured after superposing the receptor on its reference structure. This procedure delivers information about the movement of the ligand in its binding pocket. (E) The ligand conformation RMSD after superposing on the ligand plotted as a function of simulation time. This provides information about the conformational changes of the ligand.

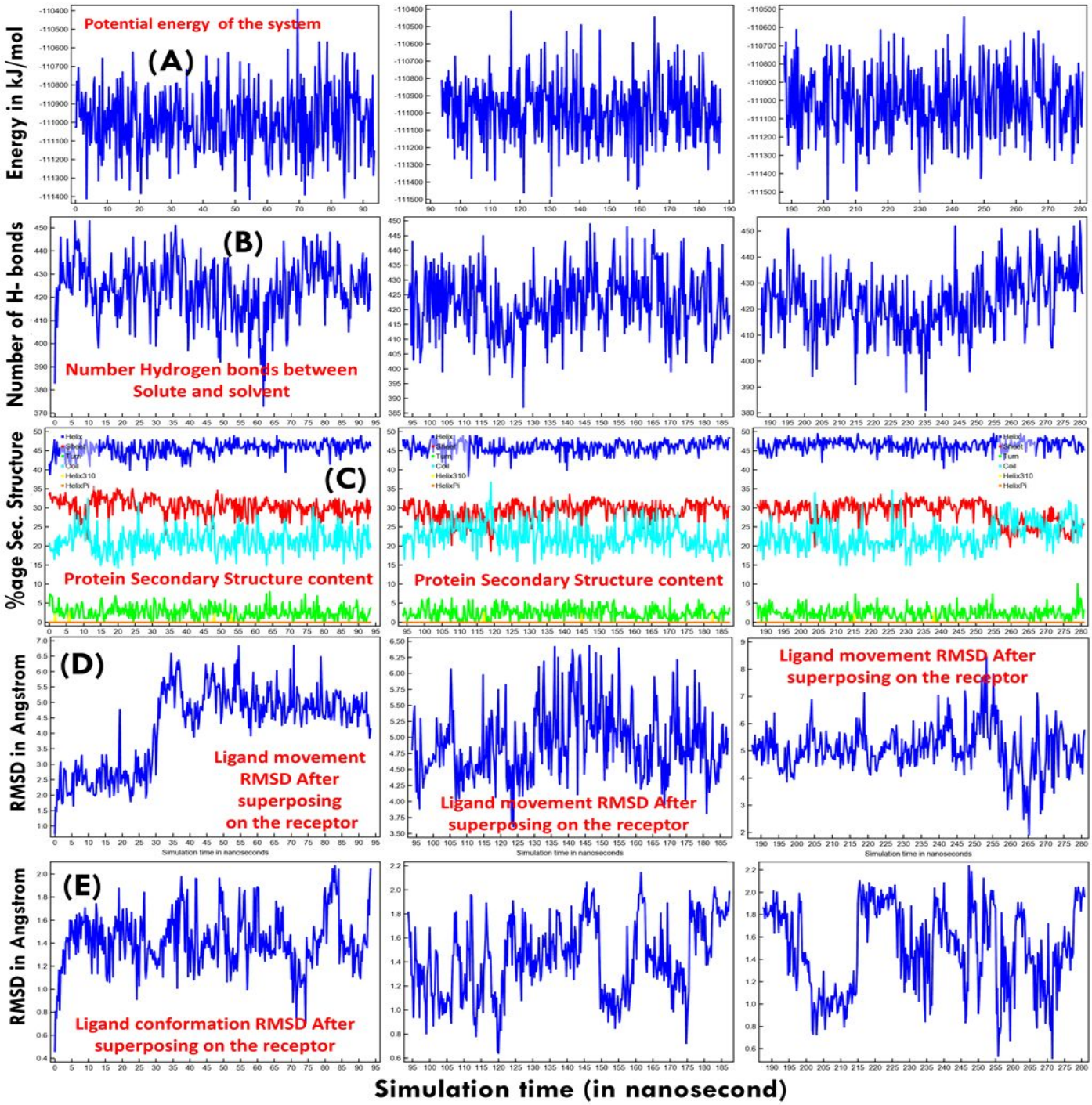

Figure S12: The results obtained from the trajectory analysis of MD simulation data on ECGC-HupD complex with highest binding energy. (A) Radius of gyration as a function of simulation time. (B) Protein RMSD from the starting structure plotted as a function of simulation time. (C,C') The plot shows time evolution of number of contacts per residue as to see how densely a certain residue range is packed and allows identifying structurally very important residues. (D) The protein residue-wise root mean square fluctuation (RMSF) calculated from the average RMSF of the atoms constituting the residue.

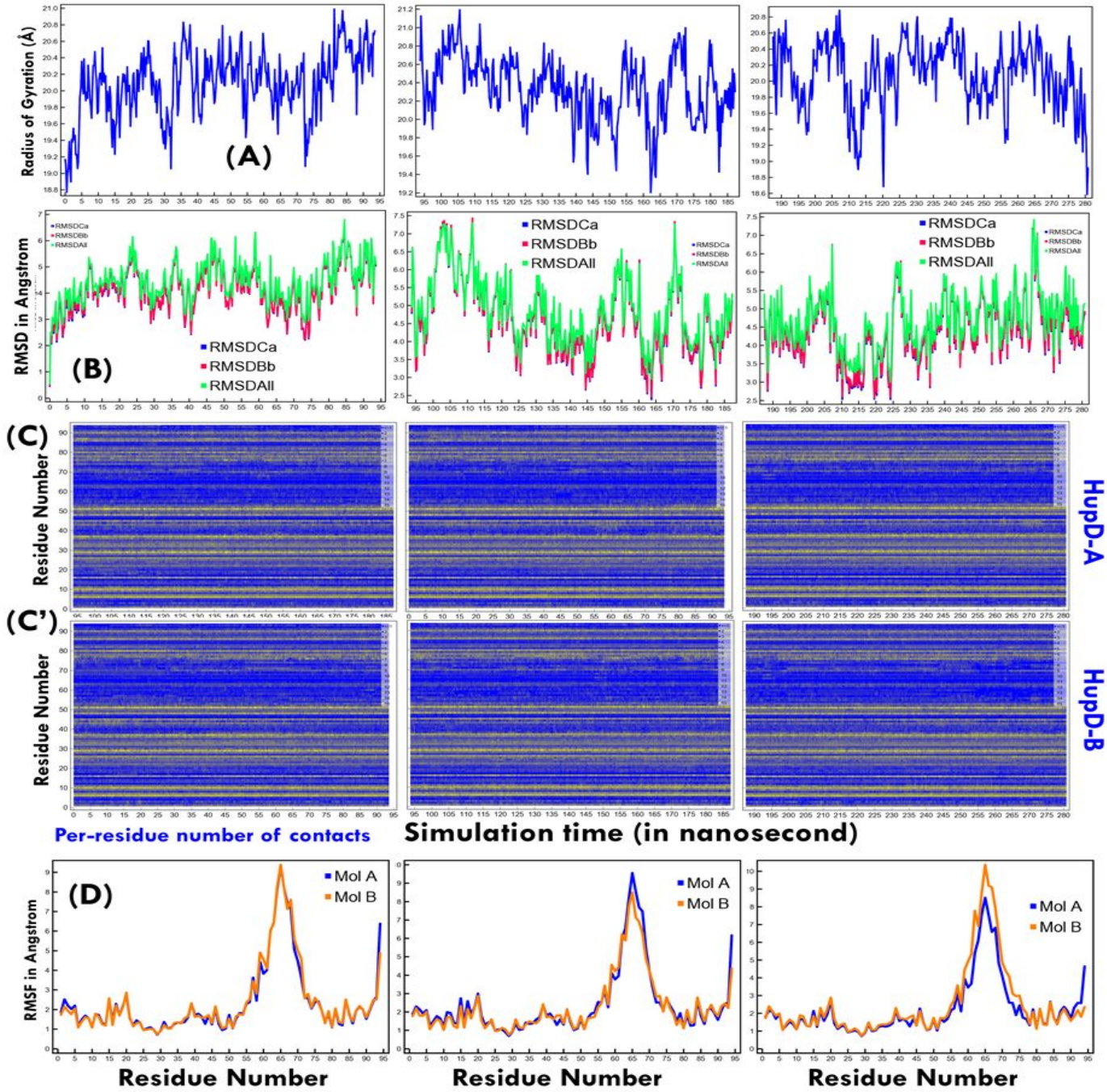

Figure S13: Time evolution of protein residue secondary structure type during the MD simulation (trajectory analysis was performed in three blocks): (A) Chain-A of HupD in complex with EGCG, (B) Chain-B of HupD in complex with EGCG, (C) Highest energy complex of EGCG with HupM and (D) second highest energy complex of EGCG with HupM.

.

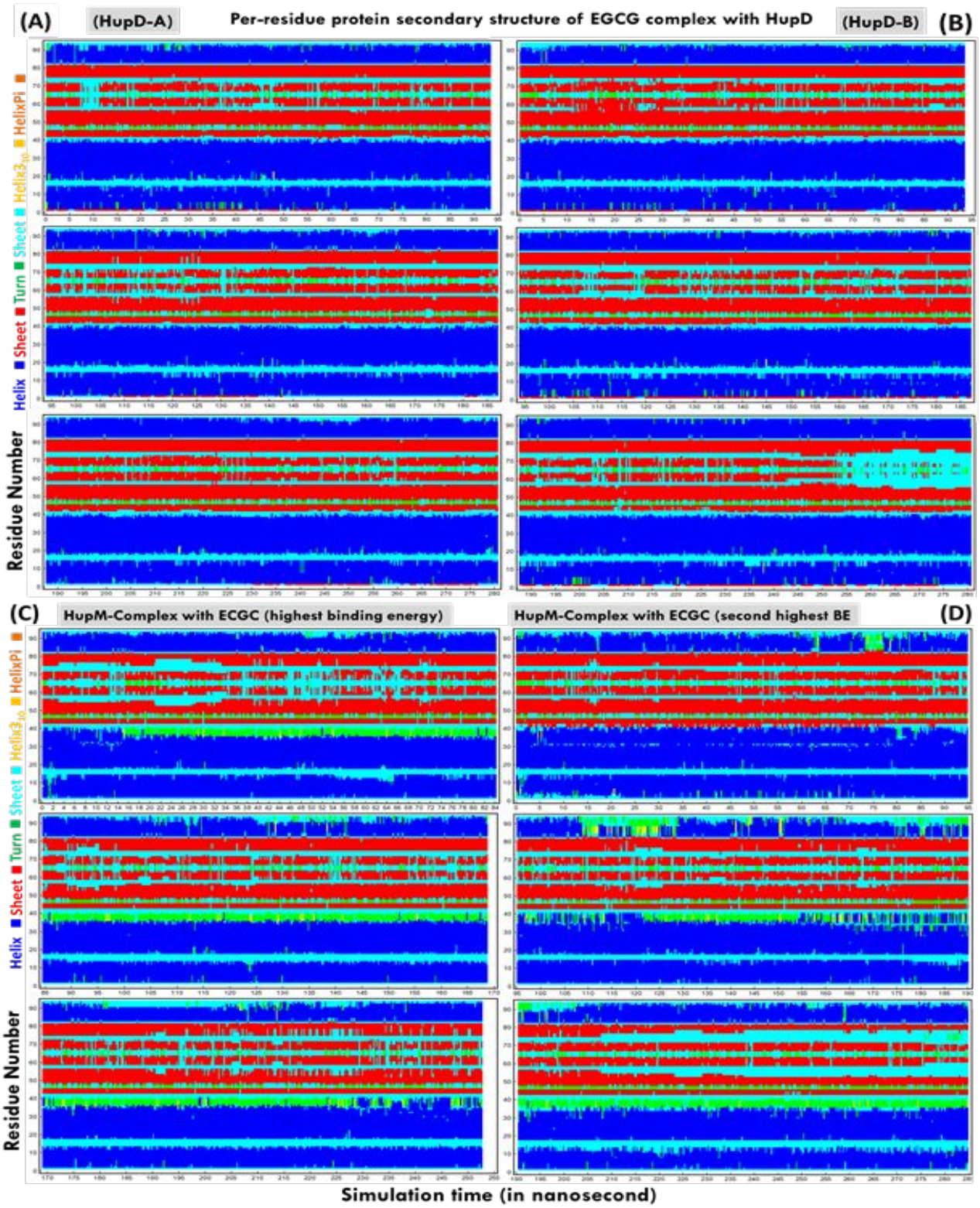

Appendix-II: ^{1}H and ^{13}C NMR Assignment of Epigallocatechin-Gallate (EGCG):

All experiments were performed on a Bruker Avance (III) 800 MHz NMR spectrometer equipped with a 5 mm inverse detection cold probe and an actively shielded z-gradient and operating at ^{1}H frequency of 800 MHz and ^{13}C frequency of 200 MHz. All spectra were measured at temperature of 300 K using 100% D_2O as solvent. The conventional one dimensional (1D) ^{1}H (at 800 MHz frequency) and ^{13}C (at 200 MHz frequency) NMR spectra were recorded using the standard pulse programs from Bruker library. The various acquisition parameters and the names of the Bruker pulse programs are summarized in Table S2.

Table S2: The acquisitions and processing parameters used for NMR experiments performed to confirm the resonance assignment of Epigallocatechin-Gallate (EGCG).

Parameters	RF pulse Offsets (ppm)	Spectral widths (ppm)	Size of FID (direct/indirect)	Zero-filling before FT	Recycle delay	Number of scans per FID
1D ^{1}H NMR (zg)	4.7	20	64 k	64 k	1.0 sec	16
1D ^{13}C NMR (zgpg30)	80	265	64 k	64 k	1.0 sec	2048

Note: RF: Radiofrequency; 1k=1024 points; 1D: one dimensional; FID: Free Induction decay

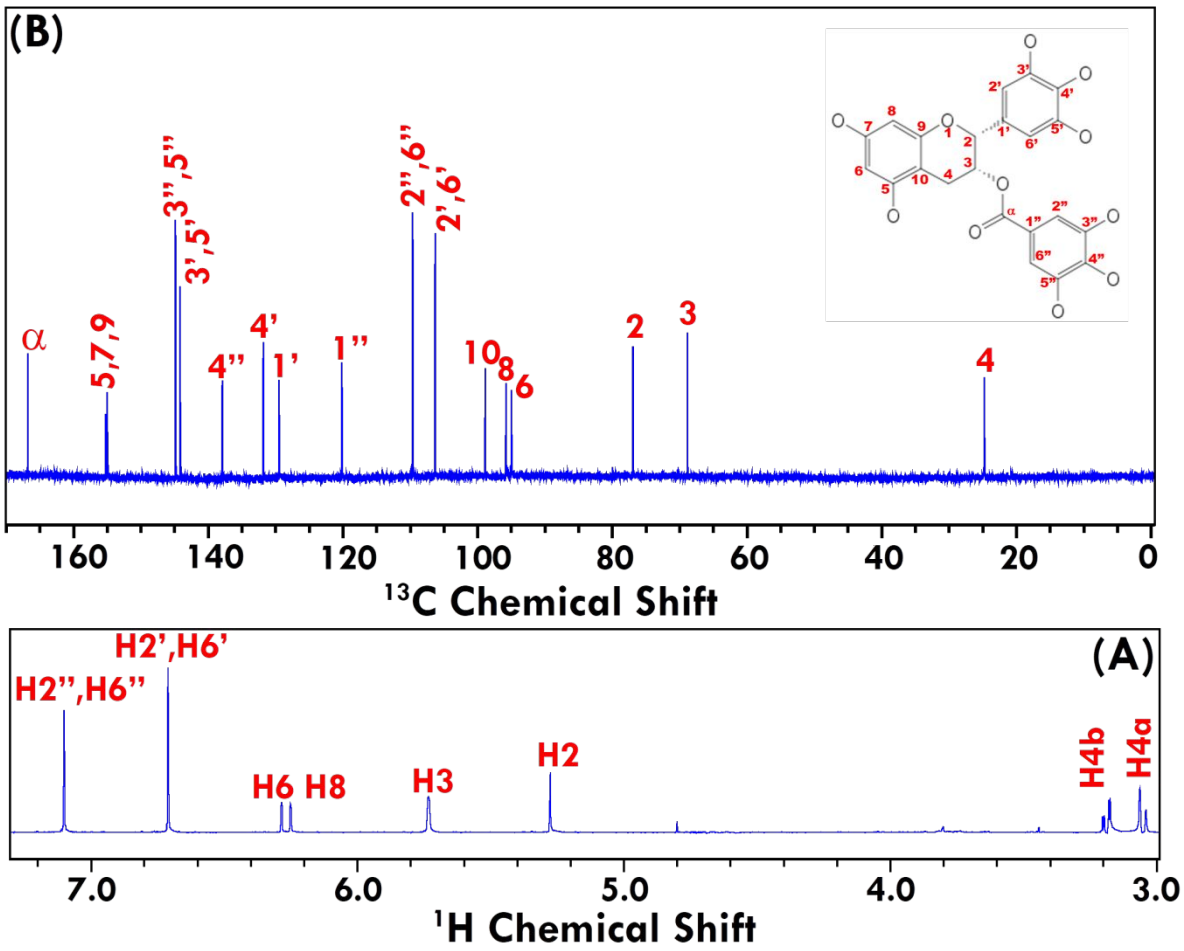

Figure S14: The 1D (A) ^{1}H NMR and (B) ^{13}C NMR spectra of purified Epigallocatechin-Gallate (EGCG, dissolved in 100% D_2O) recorded at 800 MHz NMR spectrometer.

Table S3: The NMR samples prepared for studying the interaction between Epigallocatechin-Gallate (EGCG, MW=458.37 g/mol) and Hup. The concentrations of prepared stock solutions of Hup are 600 μM (i.e. 0.6 mM) and of EGCG are 20 mM (in 100% D_2O) respectively. The final concentration of EGCG in each sample was 100 μM (also checked using UV spectrometry based on its extinction coefficient (9700 M^{-1} cm^{-1} at 280 nm).

#	NMR sample Final Volume (uL)	0.6 mM Hup Solution in uL	EGCG solution of 20mM	Sodium phosphate Buffer solution	Final Hup Conc.
1	600	0	3 μl	597	0.0 μM
2	600	4	3 μl	593	4.0 μM
3	600	8	3 μl	589	8.0 μM
4	600	12	3 μl	585	12.0 μM
5	600	16	3 μl	581	16.0 μM
6	600	20	3 μl	577	20.0 μM

Table S4A: The signal to noise ratio analysis for different NMR peaks of Epigallocatechin-Gallate (EGCG) sample (Concentration~ 100 μM) recorded in the absence and presence of Hup protein (0.0, 4.0, 8.0, 12.0, 16.0 and 20.0 μM). I_0= Ligand EGCG signal in its free form; I= Ligand signal after the addition of protein; I/I_0= normalized value; $\theta=1-(I/I_0)$ is the degree of binding; TPA: Three point average.

Hup Concentration in micromolar	Signal Intensity (I)	Initial Signal (I_0)	NS I/Io	θ (degree of binding)	Three point averaging
	EGCG Signal at 7.09 ppm				
0	474.92	474.92	1.00	0.00	0.00
4	209.34	474.92	0.44	0.56	0.44
8	118.34	474.92	0.25	0.75	0.71
12	92.05	474.92	0.19	0.81	0.80
16	81.56	474.92	0.17	0.83	0.85
20	45.31	474.92	0.10	0.90	0.87
	EGCG Signal at 6.70 ppm				
0	1178.98	1178.98	1.00	0.00	0.00
4	168.11	1178.98	0.14	0.86	0.58
8	147.29	1178.98	0.12	0.88	0.88
12	96.19	1178.98	0.08	0.92	0.91
16	70.10	1178.98	0.06	0.94	0.94
20	37.29	1178.98	0.03	0.97	0.95
	EGCG Signal at 6.28 ppm				
0	117.77	117.77	1.00	0.00	0.00
4	98.34	117.77	0.84	0.16	0.21
8	64.52	117.77	0.55	0.45	0.39
12	53.78	117.77	0.46	0.54	0.59
16	26.50	117.77	0.23	0.77	0.73
20	14.23	117.77	0.12	0.88	0.83
	EGCG Signal at 6.25 ppm				
0	110.00	110.00	1.00	0.00	0.00
4	106.86	110.00	0.97	0.03	0.12
8	72.55	110.00	0.66	0.34	0.27
12	59.91	110.00	0.54	0.46	0.51
16	30.67	110.00	0.28	0.72	0.67
20	16.82	110.00	0.15	0.85	0.78
	EGCG Signal at 5.73 ppm				
0	159.05	159.05	1.00	0.00	0.00
4	75.58	159.05	0.48	0.52	0.12
8	44.29	159.05	0.28	0.72	0.27
12	46.07	159.05	0.29	0.71	0.51
16	25.80	159.05	0.16	0.84	0.67
20	20.61	159.05	0.13	0.87	0.78

	EGCG Signal at 5.27 ppm				
0	247.04	247.04	1.00	0.00	0.00
4	73.43	247.04	0.30	0.70	0.50
8	47.41	247.04	0.19	0.81	0.78
12	44.82	247.04	0.18	0.82	0.85
16	22.52	247.04	0.09	0.91	0.90
20	10.19	247.04	0.04	0.96	0.93
	EGCG Signal at 3.18 ppm				
0	181.10	181.10	1.00	0.00	0.00
4	38.36	181.10	0.21	0.79	0.55
8	23.30	181.10	0.13	0.87	0.86
12	17.08	181.10	0.09	0.91	0.90
16	11.99	181.10	0.07	0.93	0.93
20	11.33	181.10	0.06	0.94	0.94
	EGCG Signal at 3.04 ppm				
0	223.61	223.61	1.00	0.00	0.00
4	50.61	223.61	0.23	0.77	0.54
8	32.38	223.61	0.14	0.86	0.84
12	23.05	223.61	0.10	0.90	0.89
16	16.34	223.61	0.07	0.93	0.92
20	14.81	223.61	0.07	0.93	0.93

Table S4B: The average value of degree of binding (θ) estimated from the individual three point averaged values of θ) obtained for different NMR signals of Epigallocatechin-Gallate (EGCG) for evaluating the apparent dissociation constant (kD) for the interaction between EGCG and Hup.

Hup Conc. in micromolar	The degree of binding (θ) for individual signals of EGCG (in ppm) and its average value								
	7.09	6.70	6.28	6.25	5.73	5.27	3.18	3.04	Average
0	0.00	0.00	0.00	0.00	0.00	0.00	0.00	0.00	0.00
4	0.44	0.58	0.21	0.12	0.12	0.50	0.55	0.54	0.46
8	0.71	0.88	0.39	0.27	0.27	0.78	0.86	0.84	0.73
12	0.80	0.91	0.59	0.51	0.51	0.85	0.90	0.89	0.81
16	0.85	0.94	0.73	0.67	0.67	0.90	0.93	0.92	0.87
20	0.87	0.95	0.83	0.78	0.78	0.93	0.94	0.93	0.91

Note: The average values do not include the NMR signal intensities for EGCG peaks at 6.28 and 6.25 ppm because their intensity profiles were found deviating from the hyperbolic model upon saturating with protein Hup.

Appendix-Ⅲ:

Determination of the binding constant from saturation binding curve based on NMR titration experiments

For the single binding site protein ligand interaction system (i.e. for a 1:1 complex), the equilibrium involved is described according to:[14]

$$P + L \underset{k_{off}}{\overset{k_{on}}{\rightleftharpoons}} PL \qquad \text{(S3)}$$

$$k_D = \frac{[P][L]}{[PL]} = \frac{k_{off}}{k_{on}} \quad \text{(S4)}$$

where [P], [L], and [PL] are equilibration concentrations of the receptor, ligand, and the receptor-ligand complex, respectively. The size of dissociation constant (K_d) is determined by the on (k_{on}) and off (k_{off}) rates of the ligand on its target and has the units of concentration.[15] Theoretically, a value of k_D in the mM range implies an approximately 1:1000 ratio of free to bound states of ligand in an equimolar mixture of P and L and a KD in the μM range implies an approximately1:10,00,000 ratio of these states, i.e., a much more stable complex with less of the 'free' species present.

Now, the dissociation constant can be written by introducing total ligand concentration, L_{tot}, as follows:

$$k_D = \frac{[P][L]}{[PL]} \qquad \text{(S5)}$$

$$k_D[PL] = [P][L] = [P]\left(L_{tot} - [PL]\right)$$

$$k_D[PL] = [P]L_{tot} - [PL][P]$$

$$k_D[PL] + [PL][P] = [P]L_{tot}$$

$$\frac{k_D + [P]}{[P]} = \frac{L_{tot}}{[PL]}$$

$$\frac{[PL]}{L_{tot}} = \frac{[P]}{k_D + [P]} = \frac{[P]}{k_D + [P]}$$

The equation describes a hyperbola and for a ligand based NMR titration, this can be described as

$$\frac{[P]}{k_D + [P]} = \frac{[PL]}{L_{tot}} = \frac{I_0 - I}{I_0} = \theta \quad \text{(S6)}$$

Where L_{tot} is the concentration of total free ligand evaluated based on I_0 (i.e. initial signal intensity of ligand in its free form) and I is the signal intensity of ligand during the titration in the absence and presence of Hup. The derivation of above equation is based on the assumption that there is no signal contribution

from bound ligand or there is no signal attenuation of ligand due to its interaction with receptor. As both these assumptions are very crude, therefore, the estimated dissociation constants has been referred here as apparent dissociation constants.

Appendix-IV: Virtual screening of higher molecular weight (HMW) library of AHP natural compound against the protein receptor Hup

Table S5: The binding energy parameters derived from virtual screening of HMW compound library against dimeric and monomeric Hup structures employing small molecule docking approaches (AUTODOCK, VINA and Glide).

HMW Compound		AUTODOCK		VINA		Glide		Cumulative
LID	CID	HupM	HupD	HupM	HupD	HupM	HupD	Average BE
1	9852086	5.25	5.25	7.66	6.63	6.40	3.64	5.81
2	73178	8.03	8.03	7.07	7.69	6.12	10.73	7.95
3	73178	9.20	9.20	7.23	7.65	7.82	10.98	8.68
4	73568	8.79	8.79	7.05	6.99	6.93	11.70	8.38
5	73568	8.71	8.71	7.04	7.21	5.85	10.65	8.03
6	114627	8.08	8.08	6.70	7.43	7.22	7.25	7.46
7	442428	7.63	7.63	7.06	7.01	7.24	6.41	7.16
8	442439	7.09	7.09	6.89	7.28	7.37	7.73	7.24
9	5280805	8.41	8.41	6.92	7.31	7.19	9.58	7.97
10	5280805	9.11	9.11	6.97	7.33	6.78	6.48	7.63
11	5281800	7.34	7.34	6.94	6.68	7.16	6.46	6.99
12	5281847	8.83	8.83	8.57	7.09	3.85	8.90	7.68
13	5281847	9.63	9.63	8.47	7.38	3.76	5.64	7.42
14	5282153	11.04	11.04	7.00	7.31	7.28	9.84	8.92
15	5388496	11.72	11.72	7.30	8.08	0.00	5.21	7.34
16	5388496	9.94	9.94	7.84	7.85	0.00	0.00	5.93
17	6439941	9.03	9.03	7.72	6.70	6.74	4.60	7.30
18	6476333	8.06	8.06	7.21	7.80	7.78	9.27	8.03
19	10033935	10.80	10.80	7.13	7.98	0.00	12.80	8.25
20	10033935	10.33	10.33	7.01	8.09	0.00	9.36	7.52
21	16129778	2.56	2.56	4.32	5.31	0.00	15.64	3.46
22	16129778	0.79	0.79	1.56	1.43	0.00	13.56	2.52
23	24847856	4.96	4.96	4.98	6.08	6.13	6.07	5.53
24	24847856	4.61	4.61	5.06	5.30	4.87	5.93	5.06
25	44584733	9.74	9.74	8.07	8.12	0.00	0.00	5.94
26	44584733	9.78	9.78	8.04	7.95	0.00	0.00	5.92
27	71436711	5.68	5.68	6.69	5.05	5.37	6.34	5.80
28	71436711	5.50	5.50	6.65	4.96	3.87	6.28	5.46
29	101304443	5.92	5.92	6.82	5.14	5.89	7.14	6.14
30	101304443	5.36	5.36	6.77	5.10	4.72	5.58	5.48
31	101973939	7.07	7.07	7.63	6.61	6.55	8.23	7.19
32	101973939	8.26	8.26	7.78	6.76	5.35	6.37	7.13
33	162221834	11.46	11.46	6.44	7.42	5.54	14.37	9.45

34	162221834	12.27	12.27	6.56	7.59	0.60	15.20	9.08
35	448438	7.24	7.24	8.15	7.03	3.62	0.13	5.57
36	5281247	7.53	7.53	8.49	7.00	3.27	1.05	5.81
37	12112747	7.82	7.82	9.00	7.39	5.60	2.18	6.64
38	12112747	8.77	8.77	8.62	7.22	4.69	0.64	6.45
39	23634523	6.55	6.55	7.30	5.63	5.53	4.39	5.99
40	23634523	7.39	7.39	7.24	5.87	5.44	4.03	6.23
41	23634528	7.91	7.91	7.43	6.14	5.26	4.72	6.56
42	23634528	6.85	6.85	7.70	5.67	5.04	4.39	6.08

Note: LID: Internal ID of compound in the higher molecular weight library; BE: Binding energy (kcal/mol)

(A)

#	AD_BE	HupM	AHP activity
1	9.4	Luteolin-7-O-beta-D-diglucuronide	90 µg/ml
2	8.85	Terniflorin	50–100 µm
3	8.83	Gallagic acid	125.0 µg/ml
4	8.62	Punicalagin	800.0 µg/ml
5	8.6	Luteoxanthin	7.9 µg/mL
6	8.5	Rottlerin	312–625 µg/ml
7	8.4	Corilagin	4 µg/ml
8	8.24	Punicalin	125.0 µg/ml
9	7.92	Violaxanthin	> 100 µg/ml
10	7.75	Neoeriocitrin	0.625-5 (% v/v)

AD_BE	HupD	AHP activity
12.27	Gallagic acid	125.0 µg/ml
11.72	Punicalin	125.0 µg/ml
11.04	Luteolin-7-O-beta-D-diglucuronide	90 µg/ml
10.8	Ellagitannin	800.0 µg/ml
9.78	Punicalagin	800.0 µg/ml
9.63	Rottlerin	312–625 µg/ml
9.2	1,2,3,6-tetra-O-galloyl-b-D-glucose	8 µg/ml
9.11	Rutin	97.7 µg/ml
9.03	Terniflorin	50–100 µm
8.79	Corilagin	4 µg/ml

#	VINA_BE	HupM	AHP activity
1	9.003	Luteoxanthin	7.9 µg/mL
2	8.569	Rottlerin	312–625 µg/ml
3	8.485	Neoxanthin	11-27 µg/ml
4	8.153	Violaxanthin	> 100 µg/ml
5	8.066	Punicalagin	800.0 µg/ml
6	7.835	Punicalin	125.0 µg/ml
7	7.781	Fukugiside	10.8 µm
8	7.721	Terniflorin	50–100 µm
9	7.698	Cochinchinenin C	29.5 µM
10	7.66	Ginsenoside	NR/A

VINA_BE	HupD	AHP activity
8.115	Punicalagin	800.0 µg/ml
8.086	Ellagitannin	800.0 µg/ml
8.079	Punicalin	125.0 µg/ml
7.796	Isoacteoside	50–100 µm
7.692	1,2,3,6-tetra-O-galloyl-b-D-glucose	8 µg/ml
7.594	Gallagic acid	125.0 µg/ml
7.434	Neoeriocitrin	0.625-5 (% v/v)
7.394	Luteoxanthin	7.9 µg/mL
7.376	Rottlerin	312–625 µg/ml
7.326	Rutin	97.7 µg/ml

#	GS	Hup_M	AHP activity
1	7.82	1,2,3,6-tetra-O-galloyl-b-D-glucose	8 µg/ml
2	7.78	Isoacteoside	50–100 µm
3	7.37	Neohesperidin	0.625-5 (% v/v)
4	7.28	Luteolin-7-O-beta-D-diglucuronide	90 µg/ml
5	7.24	Naringin	0.625-5 (% v/v)
6	7.22	Neoeriocitrin	90 µg/ml
7	7.19	Rutin	97.7 µg/ml
8	7.16	Acteoside	15-60 µg/ml
9	6.93	Corilagin	4 µg/ml
10	6.74	Terniflorin	50–100 µm

GS	HupD	AHP activity
15.64	Tannin	125 µg/ml
15.2	Gallagic acid	125.0 µg/ml
12.8	Ellagitannin	800.0 µg/ml
11.7	Corilagin	4 µg/ml
10.98	1,2,3,6-tetra-O-galloyl-b-D-glucose	8 µg/ml
9.84	Luteolin-7-O-beta-D-diglucuronide	90 µg/ml
9.58	Rutin	97.7 µg/ml
9.27	Isoacteoside	50–100 µm
8.9	Rottlerin	312–625 µg/ml
8.23	Fukugiside	10.8 µm

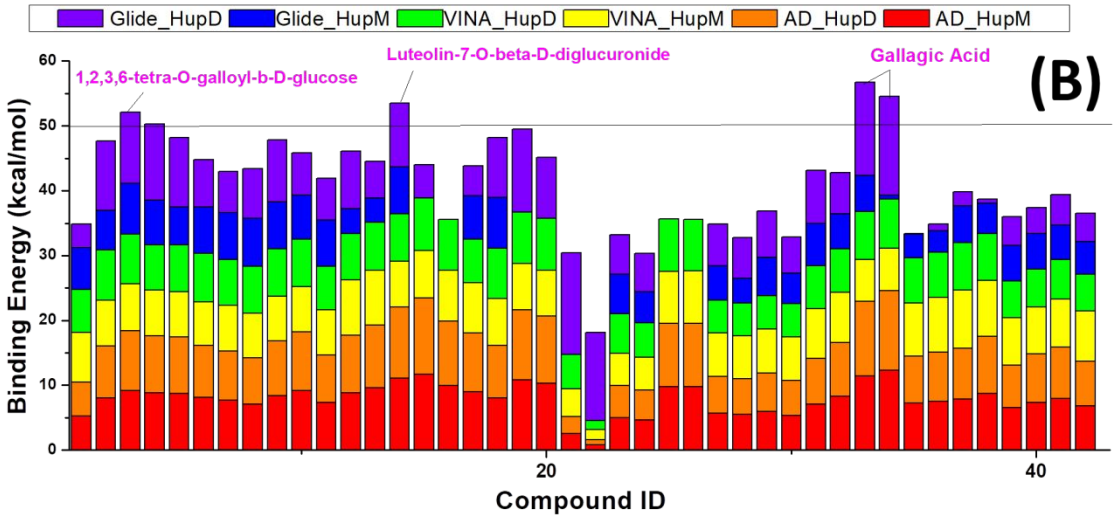

Figure S15: (A) Shows the top ten binding hits identified through AUTODOCK (top), VINA (middle) and Schrodinger glide docking using extra-precision algorithm (bottom). The different colours are used to highlight specific compounds present in top hit index. (B) Stacked binding energy (in kcal/mol) obtained after computational screening of HMW library of natural compounds against target structures of HupM and HupD receptors. The top three hit compounds i.e. Gallagic acid (LID: 33,34), Luteolin-7-O-beta-D-diglucuronide (LID: 14) and 1,2,3,6-tetra-O-galloyl-b-D-glucose (LID: 3) are highlighted in (B) and these all three were also found to be present in more than four hit indices shown in (A). Abbreviations used: AHP: Anti-H pylori; HupM: Monomeric Hup; HupD: Dimeric Hup; AD_BE: Autodock binding energy; VINA_BE: VINA binding energy; GS: glide score, LID: Internal ID of compound in Table S15.

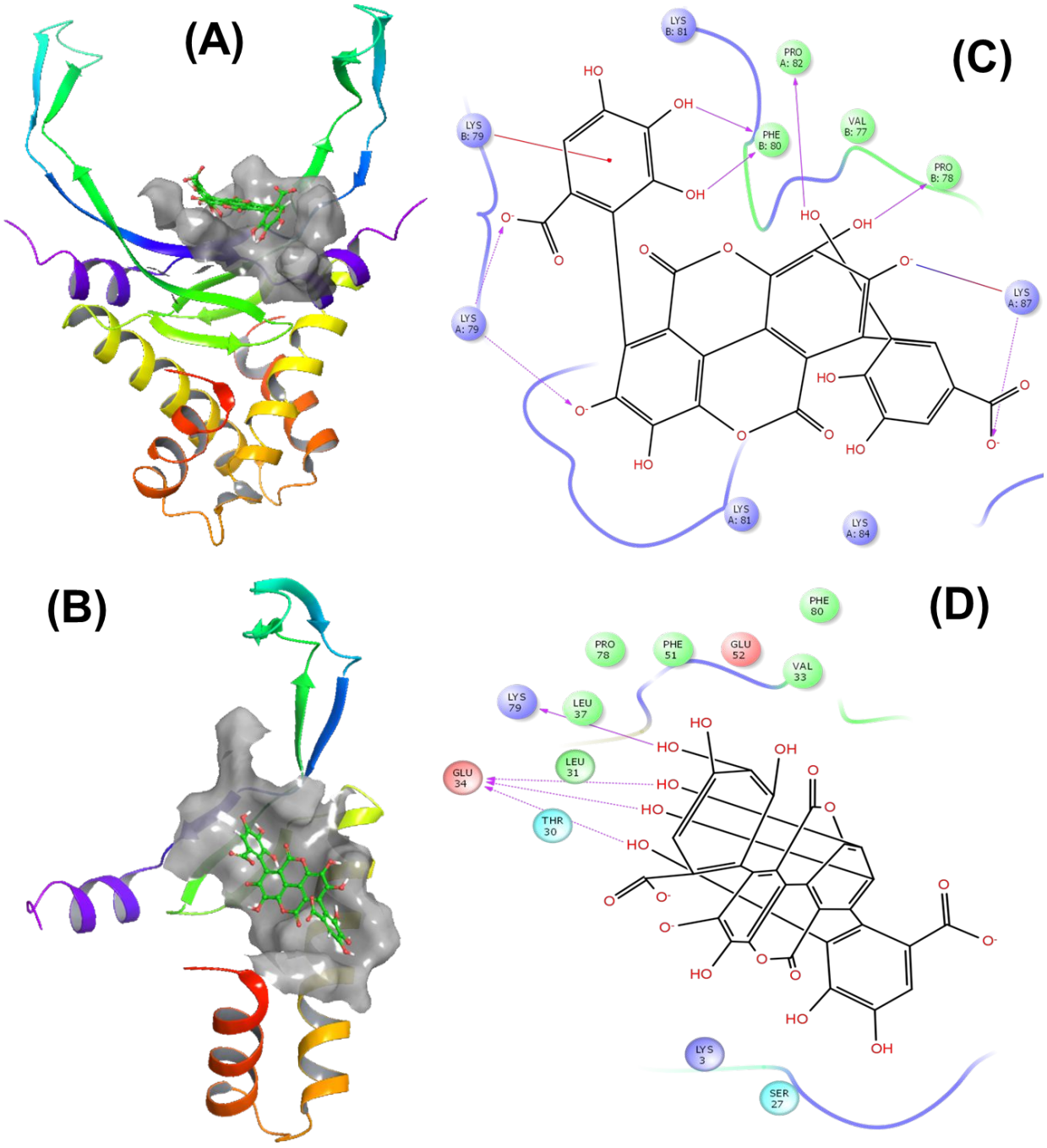

Figure S16: (A,B) The best Glide docking poses of Gallagic-acid with HupD and HupM selected after cluster analysis based on highest binding energy of the complex. (C,D) The 2D representation of molecular interaction for Gallagic acid surrounded by contacting receptor residues.

References:

1. Schrödinger, L. version 2.1. *New York, NY* 2009.

2. Raj, R.; Agarwal, N.; Raghavan, S.; Chakraborti, T.; Poluri, K. M.; Kumar, D. Exquisite binding interaction of 18β-Glycyrrhetinic acid with histone like DNA binding protein of Helicobacter pylori: A computational and experimental study. *Int. J. Biol. Macromol.* 2020.

3. Chen, C. C.; Hwang, J. K.; Yang, J. M. (PS)2: Protein structure prediction server. *Nucleic Acids Res.* 2006, *34* (suppl 2), W152-W157.

4. Chen, C. C.; Hwang, J. K.; Yang, J. M. (PS)2-v2: template-based protein structure prediction server. *BMC Bioinf.* 2009, *10* (1), 366.

5. Krieger, E.; Dunbrack, R. L.; Hooft, R. W.; Krieger, B. Assignment of protonation states in proteins and ligands: Combining pK a prediction with hydrogen bonding network optimization. In *Computational Drug Discovery and Design*, Springer: 2012; pp 405-421.

6. Dickson, C. J.; Madej, B. D.; Skjevik, +. A.; Betz, R. M.; Teigen, K.; Gould, I. R.; Walker, R. C. Lipid14: the amber lipid force field. *J. Chem. Theory Comput.* 2014, *10* (2), 865-879.

7. Hornak, V.; Abel, R.; Okur, A.; Strockbine, B.; Roitberg, A.; Simmerling, C. Comparison of multiple Amber force fields and development of improved protein backbone parameters. *Proteins: Struct. , Funct. , Bioinf.* 2006, *65* (3), 712-725.

8. Krieger, E.; Nielsen, J. E.; Spronk, C. A.; Vriend, G. Fast empirical pKa prediction by Ewald summation. *J. Mol. Graphics Modell.* 2006, *25* (4), 481-486.

9. Krieger, E.; Vriend, G. New ways to boost molecular dynamics simulations. *J. Comput. Chem.* 2015, *36* (13), 996-1007.

10. Chen, D. E.; Willick, D. L.; Ruckel, J. B.; Floriano, W. B. Principal component analysis of binding energies for single-point mutants of hT2R16 bound to an agonist correlate with experimental mutant cell response. *J. Comput. Biol.* 2015, *22* (1), 37-53.

11. Halgren, T. A.; Murphy, R. B.; Friesner, R. A.; Beard, H. S.; Frye, L. L.; Pollard, W. T.; Banks, J. L. Glide: a new approach for rapid, accurate docking and scoring. 2. Enrichment factors in database screening. *J. Med. Chem.* 2004, *47* (7), 1750-1759.

12. Friesner, R. A.; Murphy, R. B.; Repasky, M. P.; Frye, L. L.; Greenwood, J. R.; Halgren, T. A.; Sanschagrin, P. C.; Mainz, D. T. Extra precision glide: Docking and scoring incorporating a model of hydrophobic enclosure for proteinΓêÆ ligand complexes. *J. Med. Chem.* 2006, *49* (21), 6177-6196.

13. Farid, R.; Day, T.; Friesner, R. A.; Pearlstein, R. A. New insights about HERG blockade obtained from protein modeling, potential energy mapping, and docking studies. *Bioorg. Med. Chem.* 2006, *14* (9), 3160-3173.

14. Fielding, L. NMR methods for the determination of protein-ligand dissociation constants. *Prog. Nucl. Magn. Reson. Spectrosc.* **2007,** *51* (4), 219-242.

15. Becker, W.; Bhattiprolu, K. C.; Gubensäk, N.; Zangger, K. Investigating Protein-Ligand Interactions by Solution Nuclear Magnetic Resonance Spectroscopy. *ChemPhysChem* **2018,** *19* (8), 895-906.